Journal of Integrative Neuroscience

J. Integr. Neurosci. **2023**; 22(6): 143
https://doi.org/10.31083/j.jin2206143

Review

Pressure Pulsatility Links Cardio-Respiratory and Brain Rhythmicity

Owen P. Hamill[1,*]

[1]Department of Neurobiology, University of Texas Medical Branch, Galveston, TX 77555, USA
*Correspondence: ohamill@utmb.edu (Owen P. Hamill)

Academic Editor: Gernot Riedel
Submitted: 6 April 2023 Revised: 29 June 2023 Accepted: 21 July 2023 Published: 23 October 2023

Abstract

This article presents evidence indicating that intracranial pressure (ICP) pulsatility, associated with the heartbeat and breathing, is not just a source of mechanical artefact in electrical recordings, but is "sensed" and plays a role in the brain's information processing. Patch-clamp recording of pressure-activated channels, and detection of Piezo2-protein channel expression in brain neurons, suggest that these channels provide neurons with an intrinsic resonance to ICP pulsatility, which acts to synchronize remote neural networks. Direct measurements in human patients indicate that heartbeat and breathing rhythms generate intracranial forces of tens of millinewtons, exceeding by orders of magnitude the localized forces shown by atomic force microscopy and optical tweezers to activate Piezo channels in isolated neocortical and hippocampal neurons. Additionally, many human touch and proprioceptors, which are also transduced by Piezo channels, show spiking that is phase-locked to heartbeat- and breathing-induced extracranial pressure pulsations. Finally, based on the observation that low-frequency oscillations modulate the phase and amplitude of high-frequency oscillations, body and brain oscillations are proposed to form a single hierarchical system in which the heartbeat is the basic frequency and scaling factor for all other oscillations. Together, these results support the idea that ICP pulsatility may be elemental in modulating the brain's electrical rhythmicity.

Keywords: heartbeat- and breathing-induced intracranial pressure pulsatility; millinewton pulsatile forces; brain neurons; pressure-activated Piezo channels; neural network entrainment; electroencephalogram (EEG); electrical rhythmicity; proprioceptors; touch receptors

1. Introduction

Both the heart and the brain exhibit pressure pulsatility and electrical rhythmicity. For the heart, the functional link between the two is well recognized. Electrical rhythmicity drives cardiac-pressure pulsatility and the pressure-activated channels, Piezo1 and Piezo2, in the aortic arch and carotid sinus, transduce blood pressure pulsatility to modulate the heart's electrical rhythmicity via the baroreflex [1–4]. For the brain, the boney skull normally conceals its pulsatility. However, examination of a newborn's fontanelles or an adult's brain either during open-skull surgery, or under phase-based-motion-amplified magnetic resonance imaging reveals a highly dynamic pulsatile organ [5][1]. Indeed, as early as 1880, Mosso, studying adult patients with skull abnormalities, developed a technique known as plethysmography, with which he directly observed the brief cerebral-volume pulsations associated with cardiac and respiratory rhythms [6,7]. Furthermore, Mosso recorded sudden increases in slower-volume pulsations when his subjects engaged in mental activities, thereby paving the way for modern-day functional brain imaging-techniques (i.e., positron emission tomography and functional magnetic resonance imaging) that measure localized increases in blood flow known as functional hyperemia [8–11]. Still, the idea remained that the primary roles of cardiac- and respiratory-induced intracranial pressure (ICP) pulsations, were to supply the brain with oxygenated blood and eliminate waste but played no role in information processing. Instead, ICP pulsatility was more often seen as a source of mechanical artifact in recording the brain's electrical activity [12–15]. However, recent experimental observations indicate that this idea may need reconsideration. First, a patch-clamp study of mouse-brain slices showed that cerebral pyramidal neurons express single pressure-activated cation-channel currents that can promote neuronal spiking, even at the single channel current level [16]. Second, neurons in rodent and human brain express Piezo1 and Piezo2 [17–20]. Third, direct measurements in human patients indicate cardiac and respiratory rhythms generate intracranial pulsatile forces of tens of millinewtons (mN) [21], exceeding by orders of magnitude the highly localized forces known to activate pressure-sensitive and Piezo channels in isolated cells including cerebral neurons [22–26]. Based on these results, Piezo channels have been proposed to confer on central neurons a resonance with cardiac and respiratory ICP pulsations, thereby globally synchronizing remote and possibly unconnected neural assemblies [19,27]. Although this hypothesis still requires direct testing, it has already found "proof-of-concept" in studies of the human peripheral nervous system, where afferent spiking of specialized touch receptors and proprioceptors, also dependent on Piezo2 [28,29], is phase-locked to cardiac and respiratory cycles via the pulsatile mN forces generated in the surrounding tissue [30,31]. The purpose of this perspective is to review these studies and reinforce the idea that brain neurons by

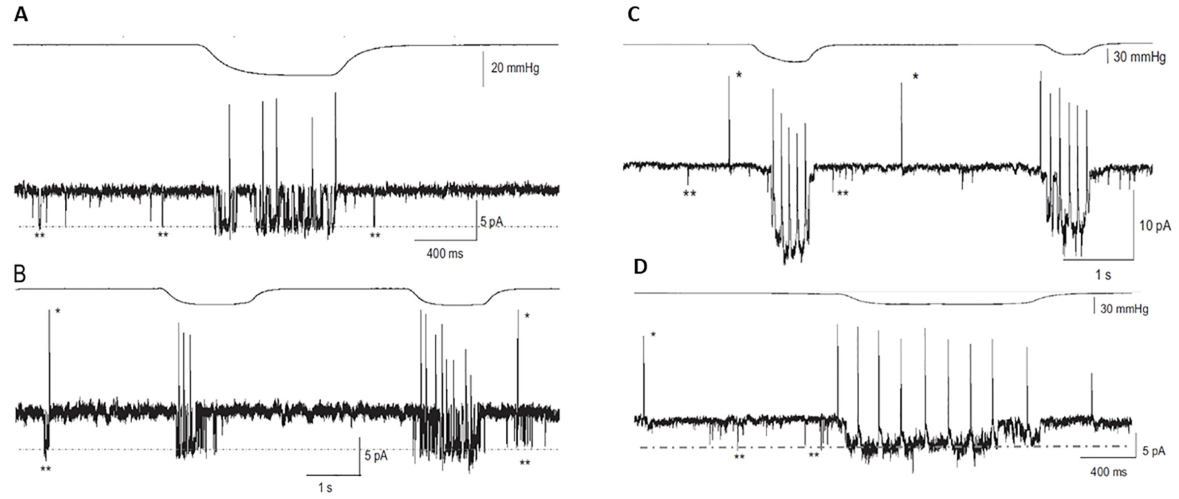

Fig. 1. Pressure-activated single channel currents trigger spiking in mouse hippocampal and neocortical pyramidal neurons. The top traces in (A–D) show the applied negative pressure pulse waveforms. (A) The lower trace is the cell-attached patch-current recorded from a mouse hippocampal pyramidal neuron indicating "spontaneous" brief (<1 ms) inward currents that displayed the same unitary amplitude (~5 pA, see dashed line) as the 20-mmHg pressure pulse activated current "bursts" that also triggered outward current spikes (i.e., action potentials in the whole neuron). (B) The lower trace is the current recorded from the same patch as in (A), with V_{pip} increased from 50 mV to 70 mV. In this case indicating that spontaneous inward channel current bursts (**) can trigger individual spikes (*). Pipette solution: divalent-free, 120 mM KCl, with an estimated single channel conductance of ~60 pS over the patch potential range of –100 mV to –120 mV. (C) The lower trace is the current recorded from a mouse neocortical pyramidal neuron. The two pressure pulses (40 and 30 mmHg) activated multiple channel inward currents (–13 pA and –10 pA) that triggered spiking (at 9 Hz and 8 Hz). (D) The lower trace is the current recorded from the same patch as in (C) with V_{pip} increased from 40 mV to 75 mV. In this case a smaller pressure pulse (20 mm Hg) activated a single channel opening that triggered 9 spikes at ~5 Hz. In both traces in (C,D) there were spontaneous spikes (*) that were not triggered by inward currents, at least as recorded in the patch. On the other hand, brief spontaneous inward currents (**) that were evident in this trace, failed to trigger a spike. Modified from Ref. [16] Brain Research, Nikolaev YA, Dosen PJ, Laver DR, van Helden DF, Hamill OP. Single mechanically gated cation channel currents can trigger action potentials in neocortical and hippocampal pyramidal neurons. 1608, 1–13, (2015), with permission from Elsevier.

transducing ICP pulsatility, provide a non-synaptic mechanism, in addition to the well-recognized synaptic mechanisms, that also communicate cardiac [32–36] and respiratory rhythms [37–43] to the brain, and thereby modulate electrical rhythmicity and behavior [44–47].

This review is organized into 10 sections with their topics briefly outlined here. Section 2: Pressure-activated channels in brain neurons. Section 3: Piezo channel gene and protein expression in brain neurons. Section 4: Peripheral baroreceptor transduction of blood pressure pulsations. Section 5: ICP pulse properties. Section 6: The pulsatile sensitivity of pressure-activated and Piezo channels. Section 7: A "proof-of-concept" in the human peripheral nervous system. Section 8: The heartbeat evoked potential and the "pulsatility artifact". Section 9: The physiology of heartbeat, breathing and brain interactions. Section 10: Cardio-respiratory rhythms linked to electroencephalogram (EEG) recorded brain oscillations. Section 11: Future challenges and *in vivo* strategies for demonstrating ICP pulsations modulate brain rhythmicity.

[1]https://directorsblog.nih.gov/tag/phase-based-amplified-mri/#:~{}:text=Recently%2C%20NIH%20funded%20researchers%20developed%20a%20video-based%20approach%20to,tiny%20movements%2C%20making%20them%20more%20visible%20and%20quantifiable

2. Pressure-Activated Channels Modulate Spiking in Pyramidal Neurons

As often happens in science [48], several of the key observations that link pressure pulsatility and brain electrical rhythmicity were unanticipated. In 1980, Neher discovered the giga-seal ("tight seal"), which was produced when he applied negative pressure to the pressure port of the patch-pipette holder to draw more membrane into the pipette [49]. Once the sudden and "unexpected" tight membrane-glass seal formed, continuing maintenance of the suction was unnecessary. However, because the seal was mechanically, as well as electrically tight [49,50], the membrane patch could be stimulated by hydrostatic or osmotic pressure gradients [51,52]. Indeed, single pressure-activated cation channels were subsequently found to be expressed almost ubiquitously in various vertebrate cell types [53,54]. More recently, utilizing the thin-slice brain technique and infrared microscopy [55,56], single pressure-

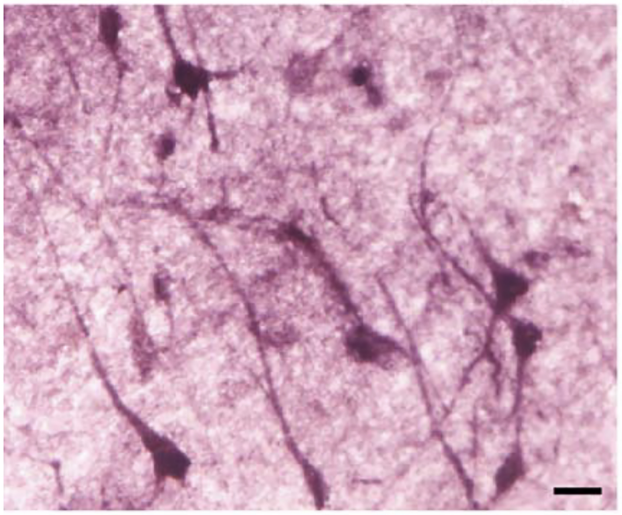

Fig. 2. PIEZO1/MIB (Membrane protein induced by β-amyloid) is expressed in pyramidal neurons of a brain from a human not suffering from Alzheimer's disease. The figure shows an in situ hybridization-stained image indicating a positive signal for *PIEZO1* mRNA transcripts in the pyramidal neurons. Scale bar: 20 µm. Modified from Ref. [18] Brain Research, Satoh K, Hata M, Takahara S, Tsuzaki H, Yokota H, Akatsu H, Yamamoto T, Kosaka K, and Yamada T. A novel membrane protein, encoded by the gene covering KIAA0233, is transcriptionally induced in senile plaque-associated astrocytes. 1108, 19–27, (2005) with permission from Elsevier.

activated cation channel currents were recorded in mouse neocortical and hippocampal pyramidal neurons [16]. Furthermore, the currents displayed channel properties (i.e., cation selectivity, single-channel conductance, inward rectification, and burst gating) like the endogenous pressure-activated cation channels reported in a wide variety of other cell types [51,57–66].

A powerful advantage of the cell-attached patch technique is that it allows simultaneous, "non-invasive" monitoring of spike activity in the whole cell [67]. In particular, the membrane patch capacitance acts to differentiate the action potential waveform, generating a typical, pronounced, outward current spike in the membrane patch. This technique has been used to record spike activity in several types of neurons [68–71] and confirm the sparse firing of neocortical pyramidal neurons in the anesthetized and awake mammalian brains [13,72]. Fig. 1A,B (Ref. [16]) show cell-attached patch recordings from a hippocampal pyramidal neuron in which brief ($\leq$1 ms) "spontaneous" inward currents displayed the same unitary current amplitude as the pressure pulse activated inward unitary currents that occurred as opening "bursts" of current and triggered spiking (Fig. 1A). Moreover, when spontaneous events did occasionally occur as longer bursts, they triggered single spikes (Fig. 1B). Recordings from neocortical pyramidal neurons showed similar behavior with multiple-activated channels triggering high-frequency spiking (Fig. 1C from [16]). Occasionally, spikes did occur independently of inward current events (Fig. 1C,D). However, it is possible that these were triggered by channel openings occurring outside the patch and therefore not recorded [16].

Previously, resting or "basal" activity of single pressure-gated channels, as seen in Fig. 1, has been proposed to arise from a significant resting tension generated by the membrane patch being "pulled flat" by tight-seal formation [73–76]. However, in the specific case of pyramidal neurons localized within the highly folded cortex, tension already exists as indicated by a rapid recoil of cut axon ends [77–80]. Moreover, vertebrate neurons, unlike many other cell types (see [74,75]) do not express microvilli or caveolae that would, by providing excess membrane, minimize any sustained membrane tension [81–83]. Given these features, basal channel activity in pyramidal neurons may provide an added source of membrane channel noise [84] contributing to the stochastic resonance proposed to occur in neocortical and hippocampal neurons [85,86]. In addition, ICP fluctuations ($\leq$5 mmHg) related to cardio and respiratory cycles (0.15–2 Hz), could have effects analogous to those of applied sinusoidal electric fields (~0.1–0.5 Hz) that phase-lock pyramidal neuron spiking with voltage fluctuations of only 1–2 mV [87,88].

3. Piezo1 and Piezo2 Expression in Brain Neurons

The membrane protein that forms the endogenous pressure-activated cation channel was discovered in 2010 by Patapoutian and colleagues, using a short interfering RNA knock-out screen to identify a novel membrane protein-channel family, which they designated Piezo [17]. Vertebrates express two family members, Piezo1 and Piezo2, shown by reverse transcription-polymerase chain reaction to be differentially expressed in various mouse tissues, including brain [17]. Significantly, cell-attached patch recordings have indicated that the single Piezo1 channel has a monovalent cation conductance of ~60 pS, like the ~60 pS channel measured in cerebral pyramidal neurons under similar divalent-free ionic conditions [16,89]. Moreover, a in situ hybridization study [18], reported that *PIEZO1*—previously identified as a gene transcriptionally upregulated in astrocytes by β-amyloid treatment—is expressed in pyramidal neurons of brains of humans not suffering from Alzheimer's disease (Fig. 2, Ref. [18]). Most recently, a study of human surgical brain tissue, using simultaneous patch clamping and sequencing (patch-seq), indicates that ~70% of layer 5 pyramidal neurons characterized, expressed *PIEZO2* transcripts, compared with ~ 50% that expressed both *PIEZO1* and *PIEZO2*; only ~10% expressed neither [20][2].

[2]https://portal.brain-map.org/explore/classes/multimodal-characterization/human-l5-et-it

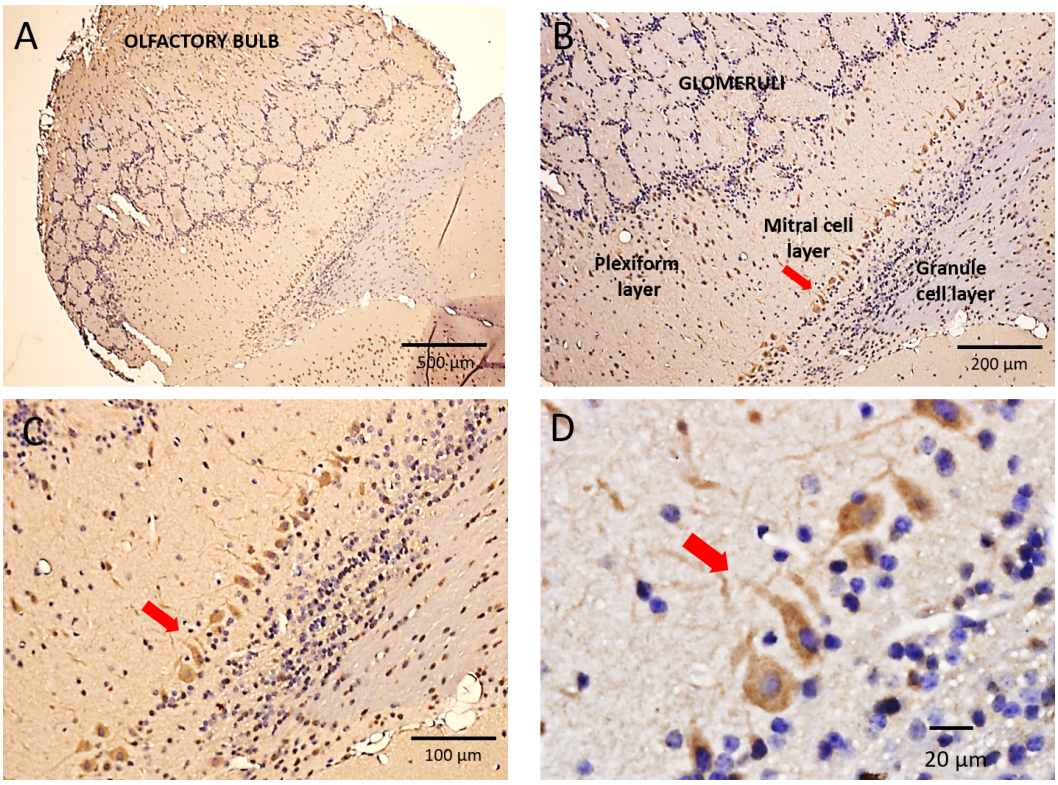

Fig. 3. Immunohistochemical localization of Piezo2 in the mouse olfactory bulb. (A) A low magnification image of the mouse olfactory bulb (OB) with its characteristic circular/spherical glomeruli structures spanning the OB. These glomeruli include the synaptic connections formed between primary olfactory nerve axons and mitral cell dendrites. (B,C) Higher magnification images (10× and 20× objectives) of the same slice showing the uniformly stained layer of mitral cell bodies (red arrows) that separate the external plexiform layer from the internal plexiform and granule cell layers. The mitral cells represent the primary projection neuron of the OB and project their axons to the piriform and entorhinal cortices and the amygdala. The external plexiform layer includes the primary and lateral dendrites of the mitral cells that extend into and throughout the plexiform layer to reach the glomeruli. Also within this layer are the cell bodies and dendrites of the tufted cells, which did not appear stained. (D) A still higher magnified image (60× objective) showing the morphology and staining of the mitral cell bodies and dendrites and the absence of staining of granule cells and the tufted cells in the granule cell and external plexiform layers, respectively. Reproduced from Ref. [19] Journal of Integrative Neuroscience, Wang J and Hamill OP. Piezo2—peripheral baroreceptor channel expressed in select neurons of the mouse brain: a putative mechanism for synchronizing neural networks by transducing intracranial pressure pulses, 20(4), 825–837, (2021).

Immunohistochemistry (IHC) has confirmed Piezo2 channel-protein expression in mouse neocortical neurons (particularly in pyramidal neurons of layers 5 and 6), hippocampal pyramidal neurons (particularly in the CA3 region), and Purkinje cells of the cerebellar cortex [19]. Moreover, human IHC studies by the Human Protein Atlas (HPA) group, using a different anti-PIEZO2 antibody, found PIEZO2 expression in neocortical and hippocampal neurons, as well as selective expression in cerebellar Purkinje cells.[3]

The Piezo2 protein expression in Purkinje cells did not express as single pressure-activated channels or pressure-induced alterations in their rhythmic spiking, even when the negative pressure (suction) pulses were increased to levels that ultimately caused patch rupture (≥100 mmHg) [16]. In this respect, the Purkinje cells were like locus coeruleus neurons that were also insensitive to suction pulses [16]. However, positive-pressure pulses were not tested as they tended to destabilize the tight seal (see [66]). This omission became more relevant when a subsequent study reported that although Piezo1 is activated by positive and negative pressures, Piezo2 is only readily activated by positive pressure [90] or whole-cell-membrane indentation [17,91]. It is worth noting that the original focus of the project [16] was to patch locus coeruleus neurons (see [92]) until on one occasion only cerebral slice-regions were preserved, and attention shifted to pyramidal neurons that express Piezo1 as well as Piezo2 [18,19].

A conceptually important and unanticipated IHC result was the selective Piezo2 expression in mitral cells of the mouse olfactory bulb (OB) (Fig. 3, Ref. [19]). At the same time, a single nucleus RNA sequencing study, also indicated *Piezo2* as a genetic marker of mouse OB mitral cells [93], and transcriptomic data on the HPA website de-

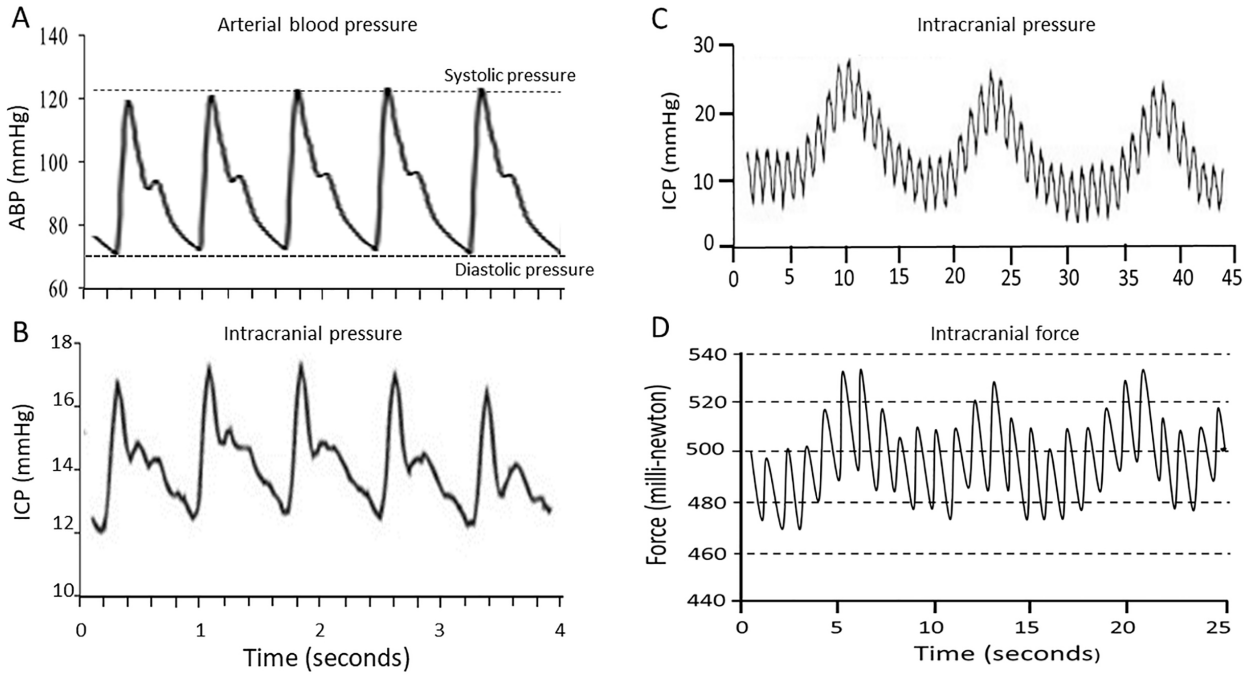

Fig. 4. Arterial pressure and intracranial pressure/force pulsatile recordings. (A) Typical arterial pressure pulse waveforms of ~40 mmHg amplitude. (B) Typical ICP pulse waveforms of ~4 mmHg amplitude measured over a short time interval of 4 s. (C) Typical ICP pulse waveforms measured over a longer time interval of 45 s indicating a fast pulse of a ~1 s that was synchronized with the heartbeat and a slower pulse of ~10 s synchronized with respiration. (D) Pulsatile intracranial force measured using implanted force transducers indicate two pulse waveforms of ~1 s and ~10 s. Data from Ref. [21] was used to generate the graph with permission of the authors: Goldberg CS, Antonyshyn O, Midha R, Fialkov JA. Measuring pulsatile forces on the human cranium. Journal of Craniofacial Surgery. 16, 134–139, (2005). ICP, intracranial pressure.

scribed *Piezo2*, as well as *Piezo1*, expression in the OB of human, pig, and mouse[4,5]. These results are significant because the OB has long been known to display an electrical rhythmicity modulated by nasal airflow [37]. Moreover, primary olfactory sensory neurons in the nasal epithelium, express, pressure-sensitive olfactory G-protein coupled receptors [94,95], this supports the idea that their afferent input to mitral cells drives the extracranial pressure sensitivity (ECP), not only of the OB, but also of other synaptically connected brain regions, including the hippocampus and neocortex [96]. Now with the demonstrated Piezo expression in mitral cells as well as cerebral pyramidal neurons, network rhythmicity may be modulated by ICP as well as ECP pulsatility [19].

[3] https://www.proteinatlas.org/ENSG00000154864-PIEZO2/tissue

[4] https://www.proteinatlas.org/ENSG00000103335-PIEZO1/brain

[5] https://www.proteinatlas.org/ENSG00000154864-PIEZO2/brain

4. Baroreceptor Neurons and their Pulsatile Pressure Sensitivity

Piezo channels are involved in a wide variety of peripheral mechanosensory functions, including somatosensation [17,28], proprioception [29,97,98], breathing [99] and blood pressure regulation [3]. Of particular interest here is their role in the regulation of blood pressure and heart rate [3,100]. The baroreceptor neurons that innervate the aortic arch and carotid sinus rapidly transduce (via Piezo1 and Piezo2) the beat-to-beat changes in blood pressure, and then, through the baroreflex, involving the vagal nerve-brain stem loop, regulate heartbeat and blood pressure [1–4]. Direct support for this role is that optogenetic activation of Piezo2 in baroreceptor neurons decreases heart rate and blood pressure, consistent with baroreflex activation, whereas genetic deletion of *Piezo1* and *Piezo2* in the neurons abolishes the baroreflex [3]. A more recent study indicates that selective deletion of *Piezo2* alone in baroreceptor neurons also eliminates the baroreflex [4]. Moreover, morphological analysis of the same neurons has indicated they form macroscopic claws that exude fine end-net endings that surround the aortic arch. This provides structural insight into how blood pressure is sensed in the arterial wall [4].

Mean arterial blood systolic and diastolic pressures are typically ~120 mmHg and ~80 mmHg, respectively, so with each heartbeat, there is also a ~40 mmHg pressure pulse of ~1 s duration (Fig. 4A, see [1]). Studies of single baroreceptor unit activity indicate a much lower threshold (i.e.,

by ~30 mmHg) for pulsatile than for static pressures [1]. In addition, dynamic pressure stimulation and pulsatile activity were shown to better augment the baroreflex [100,101]. The question then is whether the extrinsic properties of the ancillary structures (i.e., claws and fine end-net endings) or the intrinsic gating properties of the pressure activated channels (or both) determine the higher sensitivity of baroreceptors to pulsatile vs. static pressures [1,4]? This is relevant for brain neurons that express Piezo channels and presumably lack the specialized ancillary features of baroreceptor neurons, but as described next, are also exposed to pulsatile as well as steady-state ICP.

5. ICP Pulse Waveform, Pulsatile Forces Generated and Mechanism(s) of Pulse Transmission

The rigid cranium underlies the brain's extremely low compliance and limited capacity to increase in volume in response to influx of arterial blood. Consequently, brain perfusion which is a function of cerebral perfusion pressure (CPP) is determined by the difference between mean arterial pressure (MAP) and the opposing ICP (i.e., CPP = MAP – ICP). It is this relationship that motivated the development of techniques to monitor ICP in patients suffering from brain swelling due to traumatic brain injury, hydrocephalus, or cerebral hemorrhage. For example, ICP directly measured by insertion of pressure transducers into either the ventricles or the brain parenchyma, should normally show low basal levels (i.e., $<$15 mmHg see Fig. 4B,C), so that CPP is mainly determined by the MAP (~90 mmHg). However, if ICP rises above ~20 mmHg, CPP may be reduced to lethal levels [102–104]. In 1901, Cushing exploring this phenomenon experimentally, demonstrated in anesthetized dogs that elevating ICP to higher levels (i.e., $>$40 mmHg) led to a compensatory increase in MAP and thereby provided the first evidence of an intracranial baroreceptor [105]. Although this "Cushing reflex" was mostly seen as pre-terminal, subsequent studies showed that smaller increases in ICP ($\leq$10 mmHg) also increase MAP by stimulating specific regions in the lower brain stem to increase sympathetic nerve activity [106–110]. In this case, the intracranial baroreceptor acts homeostatically to maintain CPP, in opposition to the reduced MAP mediated by the extracranial baroreceptor. It is interesting that although brain stem astrocytes, rather than neurons, are implicated as these intracranial baroceptors, they may be more sensitive to the reduced arterial-oxygen tension associated with decreased perfusion of cerebral blood that accompanies increased ICP [111–113].

In addition to displaying mean baseline values, ICP also undergoes heartbeat-related pulsations similar in waveform and duration (i.e., ~1 s) to arterial blood pulsations, but with lower amplitude (i.e., $\leq$10 mmHg) (Fig. 4B, for review see [104]). Furthermore, with longer ICP recordings, slower duration pulsations (~10 s) that are synchronized with the respiratory cycle (Fig. 4C), can also be measured. Indeed, the longer duration respiratory ICP pulse allows cerebrospinal fluid (CSF) flow to build up and exceed the cardiac-induced pulsatile flow [114–116]. Specific volitional breathing practices performed to improve attention or reduce stress or anxiety and involving slow inspiration/expiration cycles or diaphragmatic vs. thoracic breathing (i.e., resonant breathing) cause even larger pulsatile changes in ICP, arising from the inspiration-induced movement of cerebral venous blood into the spinal cord, accompanied by a compensatory movement of CSF from the spinal cord back into the brain [116–118].

Other studies have used non-invasive techniques—transcranial doppler ultrasound and phase contrast magnetic resonance imaging—to measure the pulsatile nature of CSF flow and brain motions [5,104,119,120]. However, there appears to be only one study that has directly measured the pulsatile forces that generate these different pulsatile phenomena. Goldberg and colleagues [21], by inserting a force transducer into the epidural space at the periphery of a craniotomy performed on neurosurgical patients, measured two pulse waveforms—a ~1 s duration, ~30 mN pulse and a ~10 s, ~20 mN pulse—synchronized with the patient's heartbeat and ventilation rate, respectively (Fig. 4D, Ref. [21]). Given these forces plus the reported surface area of the transducer (9×10^{-6} m^2), and using Pascal's principle (i.e., Pressure = Force/Area) the ICP pulses were calculated as ~17 and ~25 mmHg, which are of the same order as measured ICP pulses (i.e., $\leq$10 mmHg) [21,104]. For comparison, pulsatile forces measured in other living tissues, were ~40 mN in the contracting pig heart [121] and ~6 mN in the human fingertip pad [30].

Another important issue regarding ICP pulsatility relates to the mechanism(s) that generate and transmit the ICP pulse throughout the brain. This has relevance because it is this ICP pulse transmission that has been proposed to rapidly synchronize remote neural networks [19]. During systole the arterial-blood inflow to the brain transiently exceeds the venous outflow, so that the brain experiences a transient expansion in volume. It is this volume increase that generates the ICP pulse [122]. However, the exact mechanism by which the ICP pulse is transmitted throughout the brain remains unresolved. One theory, referred to as the "acoustic transmission theory", assumes that the ICP pulse represents the arterial pressure pulse, and this is what is propagated throughout the CSF space as a traveling (or transmitted) wave, at the speed of sound in water (i.e., ~1500 m/s). In this case, the ICP pulse should be detectable almost instantaneously throughout the brain and should be synchronized with the arterial pulse [123,124]. In contrast, what is referred to as the "resonance theory" assumes a cerebral Windkessel effect prevents the direct spread of the arterial pulse (i.e., as a bolus of blood) throughout the rest of the vasculature (i.e., capillaries and veins) [125–127]. Instead, during systole the CSF links the arterial radial ex-

pansion to venous compression, and then during diastole the CSF links venous expansion to arterial relaxation. In this way, two travelling waves are created—one wave excited by an external force and another reflected by the elastic contents of the cavity—that are superimposed to create a standing wave that oscillates rather than travels (Fig. 5). It is also this CSF-mediated reciprocal, equal and opposite, venous compression and expansion that acts as a pulse absorber to protect the delicate cerebral capillaries from pulsatile forces [127]. In this respect, the cerebral Windkessel effect differs from the peripheral Windkessel effect, in which the aorta acts as an elastic buffering chamber to transiently store ~50% of the systolic stroke volume and then push it forward during diastole to create a continuous blood flow [128]. However, because of the high compliance of peripheral tissue, the elastic energy of each pulsatile aortic expansion is dissipated throughout its surroundings. This mechanism of energy dissipation cannot occur in the brain because of its extremely low compliance (i.e., each heartbeat generates only a ~1 mL expansion, or ~0.08% assuming a ~1300 mL brain volume [122]). Instead, the cerebral Windkessel's two-way arterial-CSF-venous pump generates both resonant and anti-resonant properties, ensuring efficient perfusion and capillary protection, respectively [127].

The resonance theory, not yet universally accepted [123,124], can account for several key experimental observations [127]. First, the unexpected observation that the ICP pulse can precede the arterial pulse would seem to rule out a simple transmission theory but can be explained if the brain has its own resonance properties that filter fast-frequency components of the arterial pulse, thereby creating asynchrony with the ICP pulse [127,129]. Second, at heartbeat frequency there is a low amplitude component of the ICP pulse, referred to as a "notch", which is consistent with anti-resonant behavior, and which disappears during either intracranial hypo- or hypertension, presumably because the anti-resonant effect is lost under both abnormal conditions [127,129]. The resonance theory raises several questions in relation to possible ICP pulse synchronization of neural networks. First, does the standing wave collapse between cardiac pulses, and if so, what are the consequences? This would seem particularly important when pulse frequency is significantly slowed, perhaps most dramatically during freediving in humans to ~10 beats per minute [130,131]. Second, since standing waves are characterized by maximal and minimal pressures, referred to as antinodes and nodes, respectively (Fig. 5), do privileged regions or network hubs exist within the brain that are subjected to specific pressure domains?

6. The Dynamic Sensitivity of Pressure Activated and PIEZO Channels

Given the forces and dynamics of ICP pulsatility discussed above, the question is whether pressure-activated

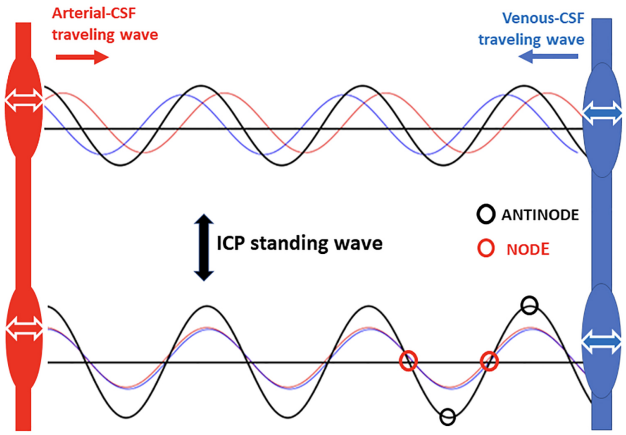

Fig. 5. Schematic representation of the ICP standing wave generated by the superposition of two traveling waves. One generated by the arterial pressure pulse perturbation of the cerebrospinal fluid (CSF) and the other a reflected travelling wave generated by the venous recoil that perturbs the CSF. The key difference with the standing wave is that it oscillates up and down without travelling and this way generate antinodes of localized high pressure and nodes of localized minimal pressure.

and Piezo channels possess the dynamic force sensitivity to transduce ICP pulsations efficiently? The development of the fast pressure-clamp enabled measurement of the rapid kinetics of single mechanosensitive channels [132–134]. Introduced before Piezo identification, it was first used to analyze the gating of the endogenously expressed pressure-activated cation channels in various cell types [133,135,136]. Fig. 6A (Ref. [75,133]) shows the transient response to stepwise increases in pressure with rapid (i.e., <100 ms) and complete channel closure, even in the presence of sustained pressure stimulation. On the other hand, the same channels can efficiently transduce continuous, sinusoidal, pressure stimulation at 0.5 Hz (Fig. 6B [133]). More recent pressure-clamp [137] and whole-cell-indentation [138] studies of Piezo1 and Piezo2 have shown that there is efficient transduction for frequencies ranging from 0.5–50 Hz [139] indicating that these channels can accurately transduce the pulsatile pressure changes associated with heartbeat (~1.5 Hz in humans; ~10 Hz in mice) and breathing rhythms (~0.2 in humans; 1–4 Hz in mice).

Estimates of pressure/force sensitivity vary with specific measuring techniques and recording conditions. Cell-attached patch recording combined with a gentle-sealing protocol [135,136], can yield maximum sensitivity, which is otherwise lost with "hard seals", overstimulation of the patch, or by membrane blebbing [135,136,140]. For example, in the patch described in Fig. 6C [75], obtained with a gentle seal, the pressure-current relations in response to brief step changes in negative and positive pressures indicated that pressures that activated half the channels (P_{50}) were –10 mmHg (–1.3 kN/m^2) and 14 mmHg (1.86 kN/m^2)

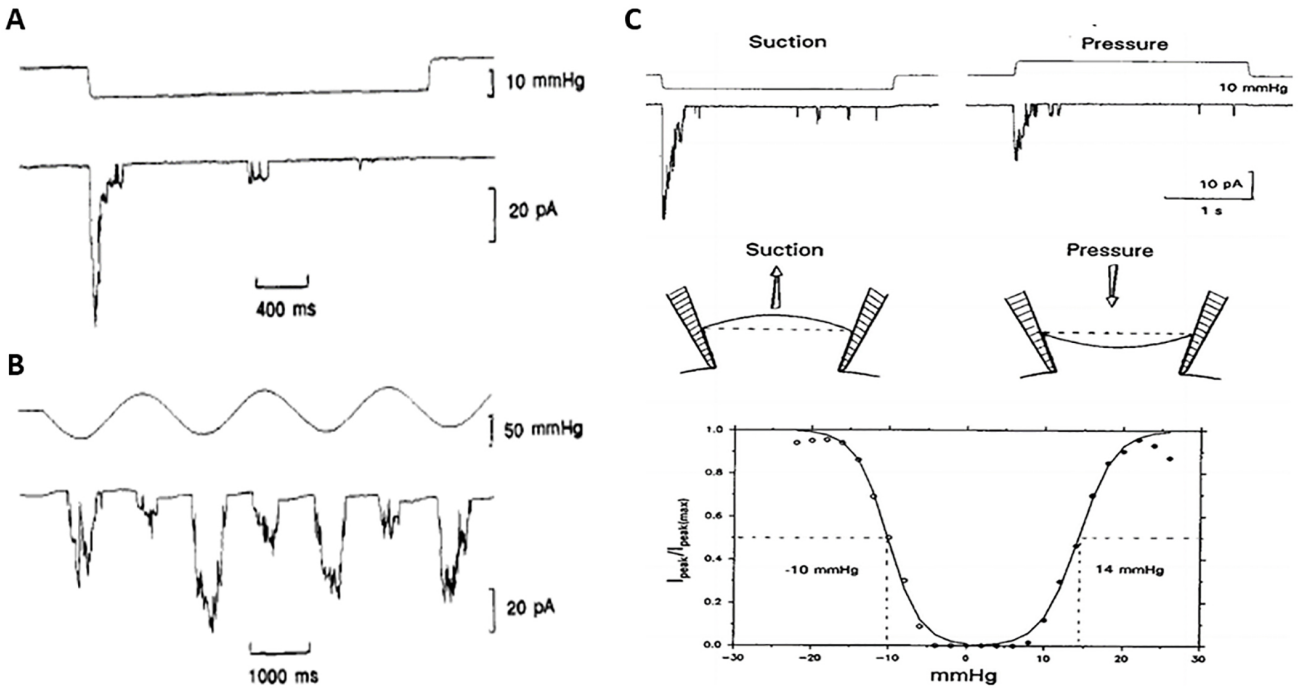

Fig. 6. Gating kinetics and pressure sensitivity of endogenously expressed pressure-activated cation channels in *Xenopus* oocytes. (A) The upper trace is the pressure step waveform (2.5 s) applied to a cell-attached patch. The lower trace is the activated channel current showing rapid channel opening (<10 ms) followed by almost complete channel closure within 200 ms even with sustained pressure stimulation. (B) A sinusoidal pressure stimulus (~0.5 Hz) applied to the same cell-attached patch as in (A). Note the asymmetry in the pressure activation of the pressure sensitive currents, with larger currents activated during negative compared with positive pressure. Nevertheless, the channel was able to efficiently transduce the repetitive stimulus for the lifetime of this patch (i.e., >5 minutes). (C) Comparison of the pressure sensitivity of the channel to suction and pressure steps. The upper traces indicate that both negative and positive pressure pulse activate rapidly inactivating currents. The middle traces indicate the symmetrical patch deformation by suction/pressure pulses based on previous high-resolution imaging of the patch. The lower panel shows normalized suction and pressure stimuli-peak current response plots. The sigmoid fits indicate that suction ($P_{0.5}$ = –10 mmHg) was slightly more effective than pressure ($P_{0.5}$ = 14 mmHg) in activating the channels. Note that increased channel activity occurred with pressures less than ±10 mmHg. (A,B) modified from [133] McBride DWJr, and Hamill OP. Pressure clamp technique for measurement of the relaxation kinetics of mechanosensitive channels. Trends in Neurosciences, 16, 341–345, (1993) with permission from Elsevier; (C) reproduced from [75] Hamill OP. "Twenty odd years of stretch-sensitive channels". Pflugers Archives, 453, 333–351, (2006) with permission from Springer Nature.

(Fig. 6C). The near symmetrical responses to suction and pressure are indications of tension-gated channels, thereby justifying the use of Laplace's law (T = 2 P/r) to estimate T_{50} tensions of 1.3 mN/m and 1.86 mN/m for a patch radius of curvature (r) of ~2 µm. A similar T_{50} of 1.4 mN/m has been reported for expressed Piezo1 channels that were measured in cell-attached membrane patches on a transfected cell line [141]. On the other hand, a significantly reduced tension sensitivity was reported for Piezo1 channels reconstituted in artificial lipid bilayers ($T_{50} \sim$ 3.4 mN/m) [142] or when expressed in cell membrane blebs ($T_{50} \sim$ 4.5 mN/m) [143], which in both cases lacked the actin cytoskeleton. However, other studies have indicated that the actin cytoskeleton is key to preserving the mechanosensitivity of endogenous and Piezo1 pressure-activated channels [22,144]. First, pretreatment of cells with F-actin disrupting agent significantly reduces the whole-cell response to surface indentation [22]. Moreover, in the same study, an optical-tweezer force of only 5.5 pN, when applied directly to the actin cytoskeleton, could activate channels; this was ~10,000 times smaller than the 50 nN force estimated for external surface-probe activation [22]. More recently, a structural link between the Piezo1 channel and actin fibers has indicated that the activating force is transmitted via focal adhesions (or integrins) to the extracellular matrix to activate Piezo1 [144]. For example, although knockdown of Piezo1, E-cadherin or β-catenin significantly reduced pressure sensitivity as did F-actin-disrupting agents, co-expression of E-cadherin and Piezo1 produced an increase in sensitivity by reducing the P_{50} value from ~45 mmHg to ~30 mmHg [144]. A further structural analysis indicated that extracellular and intracellular links with Piezo1 may allow E-cadherin to directly focus cytoskeleton-transmitted force on the Piezo1-channel-gating mechanism [144].

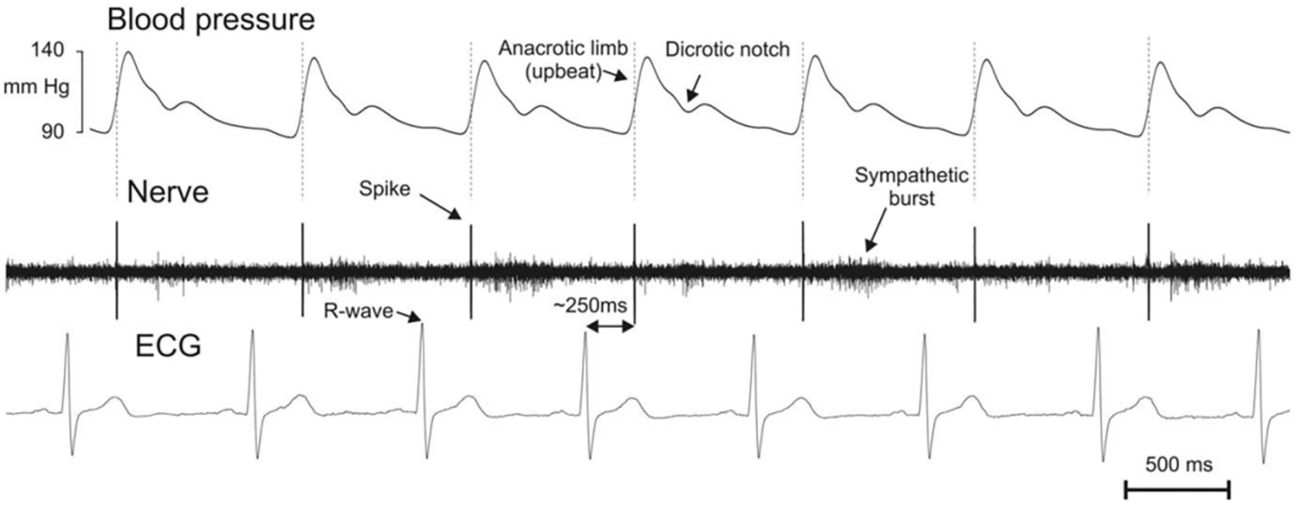

Fig. 7. Example of muscle spindle discharge locked to the arterial pressure pulsations. This afferent responded with one single spike at the early part of the upbeat of pulse wave ~250 ms following the R-peak in the electrocardiogram (ECG) signal. Note the absence of spontaneous spike activity but the indicated presence muscle sympathetic burst activity. Reproduced from Ref. [31] PLoS ONE, Birznieks I, Boonstra TW, Macefield VG. "Modulation of Human Muscle Spindle Discharge by Arterial Pulsations - Functional Effects and Consequences". 7(4), e35091, (2012) with permission from John Wiley and Sons.

Two recent studies have specifically measured the pressure/force required to stimulate neocortical and hippocampal neurons that were grown in tissue culture [24,26]. In one case, an oscillating fluid shear stress of only 1–5 Pa (0.0075–0.038 mmHg) activated intracellular Ca^{2+} ($[Ca^{2+}]_i$) transients with a rise time of ~1 s and an exponential decay time constant of ~2.5 s [24]. Significantly, even in the absence of shear stimulation, neurons showed spontaneous $[Ca^{2+}]_i$ transients of similar amplitude and kinetics. Moreover, both the spontaneous and shear induced responses were blocked by removal of extracellular Ca^{2+} and were abolished by selective blockers of voltage-gated Na^+ and Ca^{2+} channels. *Grammostola* mechanotoxin #4 (GsMTx-4), a Piezo channel blocker, partially blocked the transients, whereas transient receptor potential vanilloid (TRPV) channel antagonists caused a more complete block. One possibility is that spontaneous events arise from random channel openings that trigger spiking, as seen in Fig. 1 [16], as this would be consistent with their sensitivity to the voltage-gated channel blockers. However, the patch-clamped channels displayed the inward rectification of Piezo channels [16,89] rather than the outward rectification of TRPV channels [145,146], indicating that the exact mechanism(s) of shear force transduction remains to be defined.

In the same study [24], but using atomic force microscopy (AFM) to apply a highly localized indentation force of 100 nN to the neuron soma, global $[Ca^{2+}]_i$ transients in ~50% of neurons were activated. Those neurons also showed spontaneous $[Ca^{2+}]_i$ transients. However, the pharmacology of the AFM responses was less clear-cut; removal of external Ca^{2+} or addition of tetrodotoxin only partially reduce the $[Ca^{2+}]_i$ transients, whereas addition of GsmTx4 was without effect [24]. Nevertheless, comparing the AFM and the patch- clamp results, a 100 nN AFM force, applied with a 5 µm diameter bead, exerted an indentation pressure of 20 mmHg [24], which is the same pressure that activated single channel currents in the hippocampal pyramidal neuron patch described in Fig. 1A [16].

In the study that focused on cultured hippocampal neurons [26], an oscillating optical trap that indented the neuron with forces as low as 13 pN, activated $[Ca^{2+}]_i$ transients or whole-cell current responses. In this case, either the removal of external Ca^{2+} or the addition of GsMtx4 significantly reduced the responses. A ~10 pN force producing a ~300 nm indentation can be calculated to involve a pressure of only ~5 Pa or ~0.04 mmHg [26]. Clearly, these extremely low activating pressures/forces contrast with the AFM [24] and patch-clamp results [75] indicating that only a tiny fraction of the force/displacement required with these techniques is required to open the channels. However, although pN forces may arise as intracellular generated forces, focused by extracellular matrix molecules [144], the external forces/displacements that cells experience under physiological conditions are much larger. For example, most dorsal root ganglion (DRG) neurons only respond to indentations greater than 1 µm [147], and the most sensitive touch sensation in humans typically requires skin indentations of 10–40 µm [148]. Furthermore, as already described, the physiologically relevant pulsatile forces that mechanoreceptors experience in the human brain and fingertips are in the mN range [21,30].

7. Human Touch and Muscle-Stretch Receptor Spiking is Phase Locked to Cardio-Respiratory Related Pressure Pulsations

Touch receptors in the skin are highly specialized to transmit information to the central nervous system (CNS) about the forces exerted by the "tactile world", whereas stretch receptors located within intrafusal muscle fibers are specialized to transmit information on the exact position and movement of the body in space. However, Macefield and colleagues [30,31] have also shown that both mechanoreceptors respond to the local pressure pulsations associated with heart and breathing rhythms. Specifically, the spike discharge of many human fingertip touch receptors (~50%) and human muscle stretch mechanoreceptors (~60%) are either phase locked or modulated by the arterial pressure pulsations generated within the local vascularized tissue [30,31]. Fig. 7 (Ref. [31]) shows recordings from a human muscle spindle that indicate that a spike is activated with each heartbeat in the absence of any other spontaneous spike activity [31]. Moreover, the authors also found that the discharge of a smaller proportion (10%) of spindle afferents displayed respiratory modulation ([31], see also [149,150]). The exact role, if any, of this physiological noise that is transmitted to the CNS via the somatosensory and propriosensory neural pathways, remains unclear. Perhaps the noise is filtered out or ignored by the CNS as an interference during perception. However, arterial pulsations by acting to synchronize a barrage of afferent incoming spikes within a narrow time window (i.e., $<$100 ms) could also serve to amplify the postsynaptic depolarization of central synapses that is produced by sporadically arriving spike inputs [31]. This mechanism may be analogous to stochastic resonance, in which applied external noise increases mechanoreceptor sensitivity [151,152] and could also serve as an additional component of the "intrinsic stochastic resonance" operating on pyramidal neurons via spontaneous synaptic inputs [153–155]. A recent study has indicated that tactile sensation is higher during diastole than during systole, with a minimum at 250–300 ms after the R-peak of the electrocardiogram, which would correspond to the pulse wave arrival in the finger [156]. On the other hand, it is highest during the first quadrant after the onset of expiration [156]. Therefore, the exact mechanism by which cardio-respiratory rhythms alter conscious tactile perception remains to be determined.

Several key features of peripheral mechanoreceptor spike entrainment by cardio-respiratory rhythms [30,31] have provided "proof of concept" that Piezo2-dependent cardio-respiratory entrainment may also occur in brain neurons [19]. First, Piezo2 channels underlie mechanotransduction in both touch [17,28] and muscle stretch receptors [29,97,98]. Second, the arterial pulsatile force that activates Piezo2 in the human fingertip pad was measured at ~6 mN [30], which is significantly smaller than the measured cardio-respiratory-induced intracranial pulsatile forces of 20–30 mN [21]. Third, like the human finger pad [157] the human brain is highly vascularized with most neurons located close to ($<$100 µm) a pulsating vessel [158]. Finally, although there is a much higher density of Piezo2 channels in peripheral DRG neurons than in central neurons [19,159,160], this is to ensure a high safety factor for spike discharge by minimal (i.e., threshold) external/environmental forces. On the other hand, a lower Piezo2 density in brain neurons may serve a more subtle role of reinforcing spike entrainment that is also promoted by afferent sensory inputs related to the heartbeat and breathing rhythms [32–43].

8. The Heartbeat Evoked Potential and the "Pulsatility Artifact"

The heartbeat evoked potential (HEP) is measured by averaging brief time segments of scalp electroencephalogram (sEEG) or intracranial EEG (iEEG) recordings, time-locked to the heartbeat, usually the R peak of the electrocardiogram [14,15,32]. The neural pathways transmitting the HEP to the brain begin with a variety of Piezo-dependent mechanoreceptors that sense pulsatile changes in the heart, arteries, skeletal muscle, and skin of the chest wall [161]. The afferent output of the mechanoreceptors is transmitted mainly by the vagus nerve [162], but also by glossopharyngeal and spinal nerves, to the brainstem and thalamus; from there they are sent to higher brain regions including the central autonomic network (i.e., insula, amygdala, anterior cingulate and hypothalamus) and somatosensory cortices [163–165] with the HEP arriving 50–550 ms after each heartbeat [166–168]. The central autonomic network is notable for its control over preganglionic sympathetic and parasympathetic motoneurons [163].

The HEP, although similar in several ways to other sensory evoked potentials, is also significantly different. First, for the brain the HEP is ever-present, from gestation to death, and therefore must be considered a constant component of the brain's intrinsic electrical activity. Second, the HEP does not perform a sensory role, in that the person is usually not conscious of the heartbeat. Instead, because the HEP impacts widely spaced neural networks [163–168], it functions more in creating a "global moment" involving perception, emotion, cognition, and self-consciousness [33–36]. Indeed, changes in psychological properties, including attention, emotion, empathy, and cognition are reflected in modulation of the recorded HEP [168]. Therefore, the HEP does not function to convey cardiac-related information to the brain, but rather to modulate specific brain-network activity and functional connectivity [35]. For example, the HEP response is not generated by a simple summing of individual HEP responses, but rather by promoting phase-resetting of ongoing intrinsic neural activities [14,15].

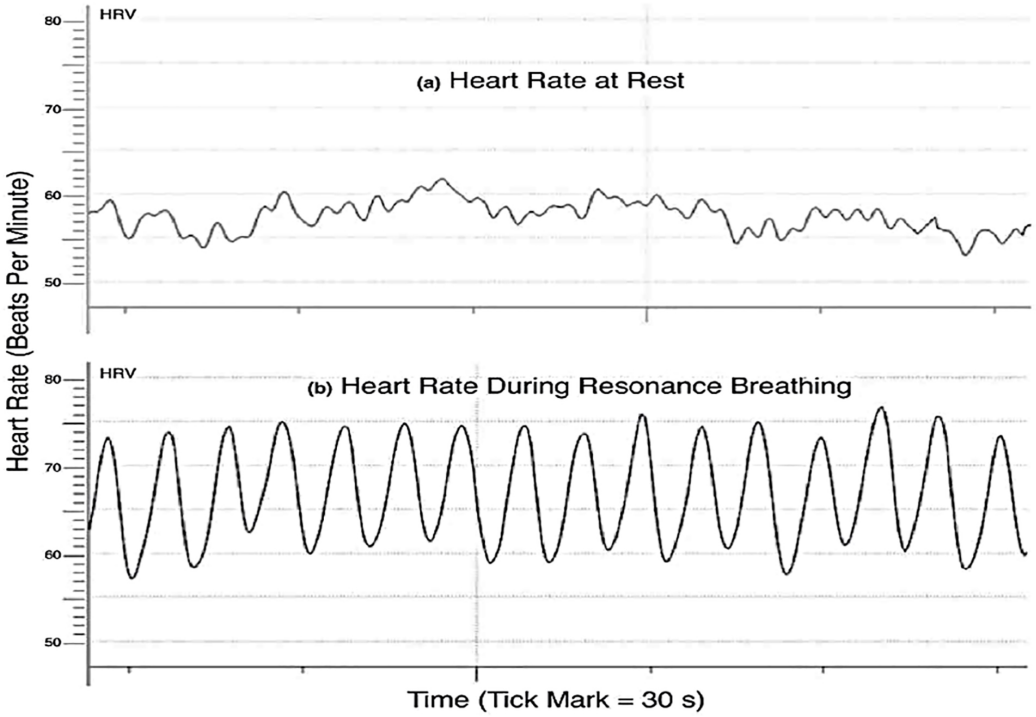

Fig. 8. Heart rate (Beats Per Minute) during normal and resonance breathing. (a) An example of heart rate variability during about a 2.5 min period during quiet rest. (b) The same person's heart rate during resonance breathing during another 2.5 min period. Reproduced from Ref. [35] Current Opinion in Behavioral Sciences. Mather M, and Thayer J. "How heart rate variability affects emotion regulation brain networks". 19, 98–104, (2018) with permission from Elsevier.

Another feature of the HEP, and most relevant for this discussion, is the so called "pulsatility artifact" that is typically seen as a HEP contaminant by causing mechanical displacement of electrodes to alter their impedance and recorded HEP [14]. Consistent with this idea, is that the pulsatility artifact is much larger (i.e., ~6×) during iEEG than during sEEG. However, the pulsatility artifact recorded at specific iEEG electrodes does not necessarily correlate with the proximity of the electrodes to large pulsating blood vessels [14]. Moreover, the pulsatility artifact has also been associated with phase shifts or synchronization of specific neural oscillations, or both (mostly <4 Hz). But in contrast to the HEP, has been labeled as artifact-evoked phase synchrony that produces only pseudo changes in neural network functional connectivity [14]. On the other hand, a quite different view is that the vascular pulsatility is functionally coupled to neural activity in a process referred to as vascular-neural coupling (VNC), the reverse of the neurovascular coupling (NVC) underlying functional hyperemia and the brain imaging techniques positron emission tomography/functional magnetic resonance imaging (PET/fMRI) [169,170]. In VNC, the mechanical changes in the cerebral vasculature are transmitted to the surrounding brain parenchyma to alter neuronal activity. Direct support for this idea comes from a study on mouse, in which increased cerebral arteriole flow/pressure decreased pyramidal neuronal firing, whereas decreased flow/pressure increased firing [170]. However, the induced pressure changes were slow (i.e., minutes) and designed to simulate the vascular tone changes during cerebral autoregulation. Moreover, the neuronal spiking was observed not to be directly triggered by pressure changes transduced by the neurons, but rather by TRPV4-expressing vascular astrocytes that release neuroactive adenosine to modulate neuronal discharge ([170], see also [112,113]). Although this slow VNC response is seen as acting as a negative feedback and neuroprotective mechanism to dynamically modulate resting neuronal activity according to vascular tone [170], the fast pressure-activated Piezo channels in brain neurons may confer a more rapid form of VNC that is mediated by heartbeat- and breathing-induced ICP pulsations [19].

9. The Physiology of Breathing, Heartbeat, and Brain Interactions

Breathing and heartbeat, as the two major oscillatory rhythms of the body, continuously interact with each other and with the brain [32–43,171]. Breathing, unlike the heartbeat, has no intrinsic pacemaker and stops when disconnected from its central input. Also, unlike the heartbeat, breathing frequency and depth of breathing are subject to rapid and conscious alteration. However, normal breathing is also a major and constant modulator of the intervals between heartbeats (i.e., Heart rate variability (HRV)) in which HR increases with inspiration and decreases with

expiration [171–177]. This process has been proposed to maximize respiratory gas exchange [175] and is a form of HRV, specifically referred to as respiratory sinus arrhythmia (RSA), in which the maximum differences in HR (HR_{insp} – HR_{exp}) can be as large as 10–20 beats/min [35]. The mechanisms underlying RSA are not entirely understood and may involve a combination of brainstem (feedforward control), peripheral (arterial baroreflex and pulmonary stretch reflex), and mechanical (e.g., intrathoracic pressure changes that alter venous blood return to the heart) mechanisms [35]. However, a recent study using intermittent positive-pressure ventilation to suppress inspiratory drive, while maintaining the pulmonary stretch reflex, found that RSA was suppressed by ~70%, indicating that a feedforward CNS drive is the major RSA generator, with pulmonary and arterial baroreflexes playing more modulating roles ([176], see also [177]).

The functional implication of HRV is that the heartbeat is not a metronome [173]. Instead, a low HRV is seen as a sign of poor health and vulnerability to physical/psychological stressors and disease [178], whereas a high HRV is associated with emotional resilience, cognitive flexibility, and a more developed capacity to control affective, cognitive, and physiological aspects of stress [35,171–173]. Obviously, a high HRV provides the healthy heart with the potential to respond to physical and anticipatory demands. However, it is not so obvious why or how a high HRV translates into superior behavioral responses. This question may best be addressed in terms of resonant breathing, which maximizes RSA/HRV by reducing the breathing frequency from the normal 12–18 breaths/min (0.2–0.3 Hz) to a slow ~6 breaths/min (~0.1 Hz) [179,180]. In this case, the slow breathing of ~10 s per breath has the same duration as the baroreflex loop that includes ~5 s to transmit blood pressure changes to the brain, and ~5 s to transmit the output back, to alter HR and blood pressure. Consequently, during resonant breathing the baroreflex, blood pressure and respiration are all coordinated and combine to generate an HRV response that far exceeds that predicted from simple additive effects (i.e., they resonate). Fig. 8 (Ref. [35]) illustrates this dramatic resonant effect involving large (~20 mmHg) sinusoidal oscillations in HRV. Specific subjects that naturally display a high HRV show increased blood flow to brain regions involved in executive and emotional functions including the prefrontal cortex and the amygdala [35]. Therefore, one possible explanation is that the same brain regions determining improved brain functions also determine HRV, in which case high HRV may simply be a peripheral "indicator" of central functions. However, evidence against this pure indicator role is that when a high HRV is induced by resonant-breathing-biofeedback sessions, it relieves anxiety symptoms in patients suffering from depression or posttraumatic stress disorder and improves motor performance and cognitive flexibility in normal subjects [35,168,172,173]. Based on these observations, Mather and Thayer [35] proposed that resonant breathing promotes functional connectivity in those brain regions. In which case, several non-exclusive mechanisms as listed below may be involved:

(i) Increased blood-oxygen supply promoted by resonant breathing, as measured by fMRI, increases functional connectivity among specific brain regions involved in cognition and emotion [181].

(ii) Heartbeat-generated HEP (accompanied by the so-called pulsatility artifact) that resets intrinsic brain oscillations in autonomic brain regions involved in regulating emotion and cognition is increased in amplitude by resonant breathing [168,173].

(iii) Increased gain in the baroreflex that interacts bidirectionally with brainstem and forebrain regions, including those in the central autonomic network [163], that regulate arousal and parasympathetic vagal tone, specifically contributing to the anxiety-reducing effects of resonant breathing [35].

(iv) Breathing itself, particularly slow-paced and deep-nasal breathing, which has been recognized as entraining electrical oscillations in neural networks due to olfactory reafferent discharge (see below), most notably in limbic and prefrontal cortical regions [38–43].

(v) Resonant breathing by increasing the amplitude or duration of the cardio- and respiratory-related ICP pulsations [114–118] enhances (via Piezo2/ICP transduction) entrainment and functional connectivity of neural networks [19].

Regarding the last mechanism, a general synchronization and feedforward coherence has been reported between beat-to-beat ICP changes and HRV [182] and interpreted as ICP effects on the central autonomic network that regulates HRV [183]. However, whether the Piezo/ICP and/or the other mechanisms are elemental to this regulation, remains to be determined.

10. Heartbeat and Respiratory Pulsations Linked to EEG Measured Brain Electrical Oscillations

A remaining issue concerns how the heartbeat (~1.25 Hz) and respiratory rhythms (~0.25 Hz) relate to traditional brain oscillations measured by EEG (δ = 2–4 Hz; θ = 4–8 Hz; α = 8–12 Hz; β = 16–25 Hz; γ = 30–80 Hz) and seen as promoting functional connectivity within and between local neural networks [45,46]. Long-standing evidence has indicated that respiratory rhythm entrains not only the slower brain oscillations ($\leq$4 Hz) but also higher frequency ones, most notably gamma [37–43]. Those respiration-related oscillations may arise from at least three possible, non-mutually exclusive, mechanisms (see [19] for details): (a) respiratory olfactory reafferent discharge (ORD) [37–43]; respiratory corollary discharge (RCD) [38,41]; and (c) intrinsic resonant discharge (IRD). The ORD mechanism requires nasal breathing (i.e., pulsatile nasal airflow), whereas

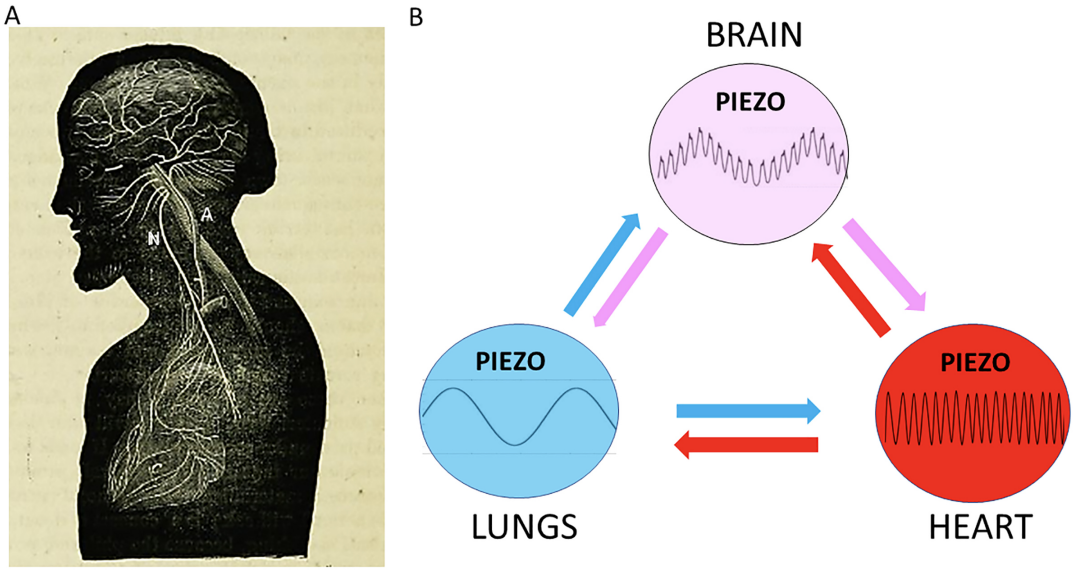

Fig. 9. Heart-lung-brain rhythms involving extracranial and intracranial pulsatile pressure cycles transduced by Piezo channels reciprocally interact. (A) An early model of heart-brain interactions represented in a drawing showing vascular (A: carotid artery) and neural (N: vagal or pneumogastric nerve) connections between the heart and brain. Reproduced from Claude Bernard's 1865 Lecture on the "Physiology of the Heart and Its Connections with the Brain" Delivered at the Sorbonne, the 27th March, 1865. Purse, 1867 [191]. (B) Schematic representing the reciprocal interactions between heart, lungs, and brain. The lung/breathing rhythm (blue) regulates the heart rate, by the process referred to as respiratory sinus arrhythmia. The heart rhythm (red) regulates lungs/breathing by a poorly understood process referred to as cardiorespiratory coupling in which peak systolic blood pressure initiates inspiration. The heart and brain interact in several ways, most notably through the baroreflex. In addition, the heartbeat evoked potential and heart rate variability impact the brain via afferent inputs to a wide range of brain regions. The lungs/breathing interact with the brain in several ways, most notably via nasal breathing that promotes respiration-related brain oscillations also referred to as respiratory olfactory reafferent discharge. Finally, it is proposed that breathing (~0.2 Hz) and cardiac (~1.25 Hz) rhythms generate ICP pulsatile cycles (pink) that synchronize neuron activity within remote neural networks via intrinsic resonance discharge.

RCD and IRD also operate during mouth breathing, with RCD dependent on inputs from brainstem respiratory centers [39,41], and IRD dependent upon ICP pulsatility [19]. A recent special topic focused on the ORD mechanism (see [184] and related articles) has provided several new insights. Most notable, is the suggestion that the respiratory-related oscillations serve as an offline mechanism (e.g., during sleep) to continually reactivate or "reignite" functionally important neuronal assemblies to counter their slow-loss overtime [185]. In this case, RCD and IRD could play a similar role. Another study addressing the species-dependent differences in breathing frequencies (i.e., 0.1–2 Hz for cats; 1–4 Hz for rats; 2–5 Hz for mice) and their effects on respiratory-related oscillations, reported that each breathing frequency modulated the amplitude of gamma oscillations of increasing frequency bands (30–60 Hz for cats; 60–100 Hz for rats and 90–130 Hz for mice) as well as synchronizing gamma oscillations in remote brain regions. These results reinforce the idea that respiration aids long-range network communication by promoting gamma oscillations whose frequencies vary with brain size [43].

Using a different approach and based on the observation that low frequency brain oscillations tend to modulate the amplitude of high frequency ones [186], Klimesch and colleagues [47,187–189], have proposed that brain and body oscillations are harmonically related, and form a binary hierarchy of center frequencies (f_i) according to the relation $f_i = s \times 2^i$, where s is a scaling factor and i = 1, 2, 3… In this case, assuming f_1 (δ) = 2.5 Hz; f_2 (θ) = 5 Hz; f_3 (α) = 10 Hz; f_4 (β) = 20 Hz; f_5 (γ) = 40 Hz, such that the next neighboring frequency was twice that of its lower neighbor. Moreover, proceeding down from the f_1 (δ) frequency, one obtains a value for f_0 of 1.25 Hz, which is assumed to be the basic frequency and corresponds to the normal, healthy-human heart rate of 75 beats/min. On this basis, HR was proposed to be the scaling factor for all brain oscillations [47,187]. Furthermore, still lower subharmonic frequencies (f_{-2} = 0.3125, and f_{-3} = 0.1565) were correlated with preferred breathing frequencies and the f_{-4}= 0.078 Hz recognized as close to the resonant breathing frequency of ~0.1 Hz [47]. This binary hierarchical theory may account for why brain oscillations are relatively preserved across species [190] despite the wide species variation in HR (e.g., 10 Hz for mouse; 1.25 Hz for man; 0.313 Hz for elephant,). For example, assuming that HR remains the basic frequency (f_0) then the order of specific brain os-

cillations could be preserved by their undergoing binary shifts within the hierarchy (e.g., $\delta = f_{-2}$, $\theta = f_{-1}$, $\alpha = f_0$, $\beta = f_1$, $\gamma = f_2$ for mouse; $\delta = f_3$, $\theta = f_4$, $\alpha = f_5$, $\beta = f_6$, $\gamma = f_7$ for elephant). The exact mechanism(s) that links body and brain oscillations remain unclear, with the possibility that ICP pulsatility and the IRD mechanism, together, play an elemental role in generating and maintaining the body-brain oscillation hierarchy.

11. Conclusions

This article has addressed evidence supporting the idea that transduction of cardio- and respiratory-induced ICP pulsations, underlies a novel, non-synaptic mechanism of information processing by the brain. However, the idea that the heart and brain are functionally linked can be traced back, at least to Claude Bernard's 1867 essay "Lecture on the Physiology of the Heart and Its Connections with the Brain" ([191], and see also [33,192]) in which he described the vasculature and pneumogastric (i.e., vagal) nerve connections between the brain and heart (Fig. 9A, Ref. [191]). Today, the two-way neural links between heart, lungs, and brain (Fig. 9B) are well recognized, and underlie several important physiological phenomena (e.g., HEP, HRV and RSA). Specifically, the mechanical oscillations of the heartbeat and of breathing are synaptically transmitted to multiple brain regions where they modulate sensory, emotional, and cognitive function [33–36,38–42,192]. Considering the multiple external neural inputs that exist, the question arises whether the proposed non-synaptic IRD mechanism has special functional significance apart from reinforcing the synaptic mechanisms. One idea is that the IRD is predominate in humans because it offers several advantages. Specifically, because the human brain is ~3250 times larger in volume than the mouse brain (i.e., ~1300 mL vs. ~0.4 mL), there may be limitations in using slow, energetic-costly, long axonal pathways to synchronize remote neural networks, particularly when compared to the advantages of synchronization by fast ICP-pulse transmission (e.g., ~1500 m/s). Moreover, the cardio-respiratory-pressure pumps provide, in addition to oxygenated blood, a "perpetual" supply of mechanical energy that the brain can utilize in the IRD mechanism. Indeed, the advantages of speed and lower energy costs have been used to argue for synchronization by electrical oscillations [45].

IRD has also been suggested to play a more significant role in humans than in other mammals because nasal breathing is not obligatory and may be volitionally switched to mouth breathing under specific circumstances. One dramatic example is human freediving, which involves respiratory-induced behavioral changes to meet the stresses of a deep dive [130]. Freedivers typically do a relaxation breathe-up, involving several minutes of slow, diaphragmatic, and exhale-biased snorkel breathing, while floating face down on the surface of the water. This practice evokes a very specific set of neurological, physiological, and psychological outcomes that allow for the exceptional experience of diving to depths as great as 200 meters [130,131]. The fact that the breathe-up involves snorkel breathing supports the idea that ICP pulsatility is what promotes the respiratory-related oscillations and the related brain state required for freediving [130]. Furthermore, once the dive commences, cardiac-induced ICP pulsatility may modulate in a top-down manner the reduction in heartbeat rate (~10 beats/min) along with the ongoing changes in sensory and cognitive functions [130,193].

The future challenge regarding the IRD mechanism remains in demonstrating that it operates *in vivo* in the CNS as convincingly as the cardio-respiratory pulse entrainment of peripheral mechanoreceptors have provided "proof-of-concept" for the IRD in the peripheral nervous system [30,31]. A somewhat similar challenge was recently successfully met using noninvasive optogenetics to evoke tachycardia, and to demonstrate enhanced anxiety-like behavior in risky contexts, confirming *in vivo* both brain and heart involvement in triggering specific emotional states [194]. However, the major challenge for the IRD mechanism is isolating its action from those of the ORD and RCD mechanisms. One obvious approach is to conduct cell-attached patch-clamp recordings from brain neurons [16] in anesthetized or awake animals [72,195]. Currently, only single unit recordings from cat and human brain using microwire electrodes have detected correlated cardio-respiratory discharge [196–198]. However, the absence of patch-clamp evidence may reflect an issue of focus rather than evidence of absence. For example, it took ~25 years after an early whole-cell patch study of neocortical pyramidal neurons [199] to test for pressure-activated channels in cell-attached patches [16].

A different approach to identify IRD mechanism in relative isolation may come from studies of ICP pulsatility in the spinal cord, particularly in lower non-mammalian vertebrates. Specifically, ICP measurements in freely moving alligators indicated sinusoidal ICP pulsations of ~60 mmHg and ~0.5 Hz that correlated with the alligator's undulated locomotion, and which disappeared when movement stopped [200]. These ICP pulses are ~15 times larger than the alligator's (and human's) cardiac-induced ICP pulsations (~4 mmHg) [200]. Those results take on added significance with the identification, initially in alligator [201] but subsequently in fish and mammal, including humans, of neurons in spinal-cord white matter that are referred to as edge cells, and which have been shown to be mechanosensitive [202–204]. Moreover, edge cells in zebra fish express Piezo2 and are proposed to act as central proprioceptors of spinal cord movement [204]. These results, and the fact that neither ORD nor RCD mechanisms should operate on spinal cord edge cells either before or during locomotion, may prove ideal in isolating Piezo2/ICP mediated IRD in the CNS.

Note Added in Proof

A recent preprint [205] by Egger and colleagues reports—using a semi-intact rat nose brain preparation and a peristaltic pump to apply arterial pressure pulsations to the cerebral vasculature—that pressure pulsations induce local field potentials within the OB, consistent with fast activation of Piezo2 channels in mitral cells. In addition, in awake animals it was found that the spiking of some mitral cells is entrained to the heartbeat, also consistent with a fast baroreceptor transduction mechanism.

Author Contributions

OPH wrote the manuscript.

Ethics Approval and Consent to Participate

Not applicable.

Acknowledgment

I thank Dr. Richard Coggeshall for critically reading the manuscript and the anonymous reviewers for their comments and suggestions.

Funding

This research received no external funding.

Conflict of Interest

The author declares no conflict of interest. Owen P. Hamill is serving as one of the Editorial Board members and Guest editor of this journal. We declare that Owen P. Hamill had no involvement in the peer review of this article and has no access to information regarding its peer review. Full responsibility for the editorial process for this article was delegated to Gernot Riedel.

References

[1] Chapleau MW, Abboud FM. Contrasting effects of static and pulsatile pressure on carotid baroreceptor activity in dogs. Circulation Research. 1987; 61: 648–658.

[2] Kumada M, Terui N, Kuwaki T. Arterial baroreceptor reflex: its central and peripheral neural mechanisms. Progress in Neurobiology. 1990; 35: 331–361.

[3] Zeng WZ, Marshall KL, Min S, Daou I, Chapleau MW, Abboud FM, *et al*. PIEZOs mediate neuronal sensing of blood pressure and the baroreceptor reflex. Science. 2018; 362: 464–467.

[4] Min S, Chang RB, Prescott SL, Beeler B, Joshi NR, Strochlic DE, *et al*. Arterial Baroreceptors Sense Blood Pressure through Decorated Aortic Claws. Cell Reports. 2019; 29: 2192–2201.e3.

[5] Terem I, Ni WW, Goubran M, Rahimi MS, Zaharchuk G, Yeom KW, *et al*. Revealing sub-voxel motions of brain tissue using phase-based amplified MRI (aMRI). Magnetic Resonance in Medicine. 2018; 80: 2549–2559.

[6] Mosso A. Sulla circolazione del sangue nel cervello dell'uomo. 1st Edition. Coi tipi del Salviucci: Roma, Italy. 1880. (In Italian)

[7] Mosso A, Raichle ME, Shepherd GM. Angelo Mosso's Circulation of blood in the human brain. Oxford University Press: Oxford. 2014.

[8] Raichle ME, MacLeod AM, Snyder AZ, Powers WJ, Gusnard DA, Shulman GL. A default mode of brain function. Proceedings of the National Academy of Sciences of the United States of America. 2001; 98: 676–682.

[9] Logothetis NK, Pauls J, Augath M, Trinath T, Oeltermann A. Neurophysiological investigation of the basis of the fMRI signal. Nature. 2001; 412: 150–157.

[10] Hennig J, Kiviniemi V, Riemenschneider B, Barghoorn A, Akin B, Wang F, *et al*. 15 Years MR-encephalography. Magma. 2021; 34: 85–108.

[11] Zago S, Ferrucci R, Marceglia S, Priori A. The Mosso method for recording brain pulsation: the forerunner of functional neuroimaging. NeuroImage. 2009; 48: 652–656.

[12] Fee MS. Active stabilization of electrodes for intracellular recording in awake behaving animals. Neuron. 2000; 27: 461–468.

[13] Margrie TW, Brecht M, Sakmann B. *In vivo*, low-resistance, whole-cell recordings from neurons in the anaesthetized and awake mammalian brain. Pflugers Archiv: European Journal of Physiology. 2002; 444: 491–498.

[14] Kern M, Aertsen A, Schulze-Bonhage A, Ball T. Heart cycle-related effects on event-related potentials, spectral power changes, and connectivity patterns in the human ECoG. NeuroImage. 2013; 81: 178–190.

[15] Park HD, Blanke O. Heartbeat-evoked cortical responses: Underlying mechanisms, functional roles, and methodological considerations. NeuroImage. 2019; 197: 502–511.

[16] Nikolaev YA, Dosen PJ, Laver DR, van Helden DF, Hamill OP. Single mechanically-gated cation channel currents can trigger action potentials in neocortical and hippocampal pyramidal neurons. Brain Research. 2015; 1608: 1–13.

[17] Coste B, Mathur J, Schmidt M, Earley TJ, Ranade S, Petrus MJ, *et al*. Piezo1 and Piezo2 are essential components of distinct mechanically activated cation channels. Science. 2010; 330: 55–60.

[18] Satoh K, Hata M, Takahara S, Tsuzaki H, Yokota H, Akatsu H, *et al*. A novel membrane protein, encoded by the gene covering KIAA0233, is transcriptionally induced in senile plaque-associated astrocytes. Brain Research. 2006; 1108: 19–27.

[19] Wang J, Hamill OP. Piezo2-peripheral baroreceptor channel expressed in select neurons of the mouse brain: a putative mechanism for synchronizing neural networks by transducing intracranial pressure pulses. Journal of Integrative Neuroscience. 2021; 20: 825–837.

[20] Kalmbach BE, Hodge RD, Jorstad NL, Owen S, de Frates R, Yanny AM, *et al*. Signature morpho-electric, transcriptomic, and dendritic properties of human layer 5 neocortical pyramidal neurons. Neuron. 2021; 109: 2914–2927.e5.

[21] Goldberg CS, Antonyshyn O, Midha R, Fialkov JA. Measuring pulsatile forces on the human cranium. The Journal of Craniofacial Surgery. 2005; 16: 134–139.

[22] Hayakawa K, Tatsumi H, Sokabe M. Actin stress fibers transmit and focus force to activate mechanosensitive channels. Journal of Cell Science. 2008; 121: 496–503.

[23] Gaub BM, Müller DJ. Mechanical Stimulation of Piezo1 Receptors Depends on Extracellular Matrix Proteins and Directionality of Force. Nano Letters. 2017; 17: 2064–2072.

[24] Gaub BM, Kasuba KC, Mace E, Strittmatter T, Laskowski PR, Geissler SA, *et al*. Neurons differentiate magnitude and location of mechanical stimuli. Proceedings of the National Academy of Sciences of the United States of America. 2020; 117: 848–856.

[25] Falleroni F, Torre V, Cojoc D. Cell Mechanotransduction With Piconewton Forces Applied by Optical Tweezers. Frontiers in Cellular Neuroscience. 2018; 12: 130.

[26] Falleroni F, Bocchero U, Mortal S, Li Y, Ye Z, Cojoc D, *et al*. Mechanotransduction in hippocampal neurons operates under localized low picoNewton forces. iScience. 2022; 25: 103807.

[27] Draguhn A. The mechanics of the brain. Journal of Integrative Neuroscience. 2022; 21: 22.

[28] Ranade SS, Woo SH, Dubin AE, Moshourab RA, Wetzel C, Petrus M, *et al*. Piezo2 is the major transducer of mechanical forces for touch sensation in mice. Nature. 2014; 516: 121–125.
[29] Woo SH, Lukacs V, de Nooij JC, Zaytseva D, Criddle CR, Francisco A, *et al*. Piezo2 is the principal mechanotransduction channel for proprioception. Nature Neuroscience. 2015; 18: 1756–1762.
[30] Macefield VG. Cardiovascular and respiratory modulation of tactile afferents in the human finger pad. Experimental Physiology. 2003; 88: 617–625.
[31] Birznieks I, Boonstra TW, Macefield VG. Modulation of human muscle spindle discharge by arterial pulsations–functional effects and consequences. PLoS ONE. 2012; 7: e35091.
[32] Schandry R, Sparrer B, Weitkunat R. From the heart to the brain: a study of heartbeat contingent scalp potentials. The International Journal of Neuroscience. 1986; 30: 261–275.
[33] Thayer JF, Lane RD. Claude Bernard and the heart-brain connection: further elaboration of a model of neurovisceral integration. Neuroscience and Biobehavioral Reviews. 2009; 33: 81–88.
[34] Park HD, Tallon-Baudry C. The neural subjective frame: from bodily signals to perceptual consciousness. Philosophical Transactions of the Royal Society of London. Series B, Biological Sciences. 2014; 369: 20130208.
[35] Mather M, Thayer J. How heart rate variability affects emotion regulation brain networks. Current Opinion in Behavioral Sciences. 2018; 19: 98–104.
[36] Azzalini D, Rebollo I, Tallon-Baudry C. Visceral Signals Shape Brain Dynamics and Cognition. Trends in Cognitive Sciences. 2019; 23: 488–509.
[37] Adrian ED. Olfactory reactions in the brain of the hedgehog. The Journal of Physiology. 1942; 100: 459–473.
[38] Yackle K, Schwarz LA, Kam K, Sorokin JM, Huguenard JR, Feldman JL, *et al*. Breathing control center neurons that promote arousal in mice. Science. 2017; 355: 1411–1415.
[39] Heck DH, McAfee SS, Liu Y, Babajani-Feremi A, Rezaie R, Freeman WJ, *et al*. Breathing as a Fundamental Rhythm of Brain Function. Frontiers in Neural Circuits. 2017; 10: 115.
[40] Tort ABL, Brankačk J, Draguhn A. Respiration-Entrained Brain Rhythms Are Global but Often Overlooked. Trends in Neurosciences. 2018; 41: 186–197.
[41] Karalis N, Sirota A. Breathing coordinates cortico-hippocampal dynamics in mice during offline states. Nature Communications. 2022; 13: 467.
[42] Brændholt M, Kluger DS, Varga S, Heck DH, Gross J, Allen MG. Breathing in waves: Understanding respiratory-brain coupling as a gradient of predictive oscillations. Neuroscience and Biobehavioral Reviews. 2023; 152: 105262.
[43] González J, Cavelli M, Mondino A, Castro-Zaballa S, Brankačk J, Draguhn A, *et al*. Breathing modulates gamma synchronization across species. Pflugers Archiv: European Journal of Physiology. 2023; 475: 49–63.
[44] Penttonen M, Buzsáki G. Natural logarithmic relationship between brain oscillators. Thalamus & Related Systems. 2003; 2: 145–152.
[45] Buzsáki G, Draguhn A. Neuronal oscillations in cortical networks. Science. 2004; 304: 1926–1929.
[46] Buzsaki G. Rhythms of the brain. Oxford University Press: Oxford. 2006.
[47] Klimesch W. An algorithm for the EEG frequency architecture of consciousness and brain body coupling. Frontiers in Human Neuroscience. 2013; 7: 766.
[48] Firestein S. Failure: Why science is so successful. Oxford University Press: Oxford. 2015.
[49] Neher E. Unit Conductance Studies in Biological Membranes. In Baker PF (ed.) Techniques in cellular physiology (pp. 1–16). Elsevier: North Holland, Sci. Pub. Ltd. 1982.
[50] Hamill OP, Marty A, Neher E, Sakmann B, Sigworth FJ. Improved patch-clamp techniques for high-resolution current recording from cells and cell-free membrane patches. Pflugers Archiv: European Journal of Physiology. 1981; 391: 85–100.
[51] Guharay F, Sachs F. Stretch-activated single ion channel currents in tissue-cultured embryonic chick skeletal muscle. The Journal of Physiology. 1984; 352: 685–701.
[52] Hamill OP. Potassium and chloride channels in red blood cells. In Sakmann B, Neher E (eds.) Single Channel Recording (pp. 451–471). Plenum Press: New York. 1983.
[53] Sachs F, Morris CE. Mechanosensitive ion channels in nonspecialized cells. Reviews of Physiology, Biochemistry and Pharmacology. 1998; 132: 1–77.
[54] Hamill OP, Martinac B. Molecular basis of mechanotransduction in living cells. Physiological Reviews. 2001; 81: 685–740.
[55] Edwards FA, Konnerth A, Sakmann B, Takahashi T. A thin slice preparation for patch clamp recordings from neurones of the mammalian central nervous system. Pflugers Archiv: European Journal of Physiology. 1989; 414: 600–612.
[56] Stuart GJ, Dodt HU, Sakmann B. Patch-clamp recordings from the soma and dendrites of neurons in brain slices using infrared video microscopy. Pflugers Archiv: European Journal of Physiology. 1993; 423: 511–518.
[57] Methfessel C, Witzemann V, Takahashi T, Mishina M, Numa S, Sakmann B. Patch clamp measurements on Xenopus laevis oocytes: currents through endogenous channels and implanted acetylcholine receptor and sodium channels. Pflugers Archiv: European Journal of Physiology. 1986; 407: 577–588.
[58] Christensen O. Mediation of cell volume regulation by Ca2+ influx through stretch-activated channels. Nature. 1987; 330: 66–68.
[59] Lansman JB, Hallam TJ, Rink TJ. Single stretch-activated ion channels in vascular endothelial cells as mechanotransducers? Nature. 1987; 325: 811–813.
[60] Franco A, Jr, Lansman JB. Calcium entry through stretch-inactivated ion channels in mdx myotubes. Nature. 1990; 344: 670–673.
[61] Lane JW, McBride DW, Jr, Hamill OP. Amiloride block of the mechanosensitive cation channel in Xenopus oocytes. The Journal of Physiology. 1991; 441: 347–366.
[62] Hisada T, Walsh JV, Jr, Singer JJ. Stretch-inactivated cationic channels in single smooth muscle cells. Pflugers Archiv: European Journal of Physiology. 1993; 422: 393–396.
[63] Hu H, Sachs F. Single channel and whole cell studies of mechanosensitive channels in the chick heart. Journal of Membrane Biology. 1996; 154: 205–216.
[64] Bowman CL, Lohr JW. Mechanotransducing ion channels in C6 glioma cells. Glia. 1996; 18: 161–176.
[65] Maroto R, Kurosky A, Hamill OP. Mechanosensitive Ca(2+) permeant cation channels in human prostate tumor cells. Channels. 2012; 6: 290–307.
[66] Soria B, Navas S, Hmadcha A, Hamill OP. Single mechanosensitive and Ca^{2+}-sensitive channel currents recorded from mouse and human embryonic stem cells. The Journal of Membrane Biology. 2013; 246: 215–230.
[67] Fenwick EM, Marty A, Neher E. A patch-clamp study of bovine chromaffin cells and of their sensitivity to acetylcholine. The Journal of Physiology. 1982; 331: 577–597.
[68] Lynch JW, Barry PH. Action potentials initiated by single channels opening in a small neuron (rat olfactory receptor). Biophysical Journal. 1989; 55: 755–768.
[69] Johansson S, Arhem P. Single-channel currents trigger action potentials in small cultured hippocampal neurons. Proceedings of the National Academy of Sciences of the United States of America. 1994; 91: 1761–1765.

[70] Perkins KL. Cell-attached voltage-clamp and current-clamp recording and stimulation techniques in brain slices. Journal of Neuroscience Methods. 2006; 154: 1–18.
[71] Alcami P, Franconville R, Llano I, Marty A. Measuring the firing rate of high-resistance neurons with cell-attached recording. The Journal of Neuroscience. 2012; 32: 3118–3130.
[72] Margrie TW, Meyer AH, Caputi A, Monyer H, Hasan MT, Schaefer AT, *et al.* Targeted whole-cell recordings in the mammalian brain in vivo. Neuron. 2003; 39: 911–918.
[73] Sokabe M, Sachs F. The structure and dynamics of patch-clamped membranes: a study using differential interference contrast light microscopy. The Journal of Cell Biology. 1990; 111: 599–606.
[74] Zhang Y, Hamill OP. On the discrepancy between whole-cell and membrane patch mechanosensitivity in Xenopus oocytes. The Journal of Physiology. 2000; 523: 101–115.
[75] Hamill OP. Twenty odd years of stretch-sensitive channels. Pflugers Archiv: European Journal of Physiology. 2006; 453: 333–351.
[76] Suchyna TM, Markin VS, Sachs F. Biophysics and structure of the patch and the gigaseal. Biophysical Journal. 2009; 97: 738–747.
[77] Van Essen DC. A tension-based theory of morphogenesis and compact wiring in the central nervous system. Nature. 1997; 385: 313–318.
[78] Xu G, Bayly PV, Taber LA. Residual stress in the adult mouse brain. Biomechanics and Modeling in Mechanobiology. 2009; 8: 253–262.
[79] Bayly PV, Taber LA, Kroenke CD. Mechanical forces in cerebral cortical folding: a review of measurements and models. Journal of the Mechanical Behavior of Biomedical Materials. 2014; 29: 568–581.
[80] Xu G, Knutsen AK, Dikranian K, Kroenke CD, Bayly PV, Taber LA. Axons pull on the brain, but tension does not drive cortical folding. Journal of Biomechanical Engineering. 2010; 132: 071013.
[81] Head BP, Insel PA. Do caveolins regulate cells by actions outside of caveolae? Trends in Cell Biology. 2007; 17: 51–57.
[82] Stern CM, Mermelstein PG. Caveolin regulation of neuronal intracellular signaling. Cellular and Molecular Life Sciences. 2010; 67: 3785–3795.
[83] Pol A, Morales-Paytuví F, Bosch M, Parton RG. Non-caveolar caveolins - duties outside the caves. Journal of Cell Science. 2020; 133: jcs241562.
[84] McDonnell MD, Ward LM. The benefits of noise in neural systems: bridging theory and experiment. Nature Reviews. Neuroscience. 2011; 12: 415–426.
[85] Yoshida M, Hayashi H, Tateno K, Ishizuka S. Stochastic resonance in the hippocampal CA3-CA1 model: a possible memory recall mechanism. Neural Networks. 2002; 15: 1171–1183.
[86] Ghori MB, Kang Y, Chen Y. Emergence of stochastic resonance in a two-compartment hippocampal pyramidal neuron model. Journal of Computational Neuroscience. 2022; 50: 217–240.
[87] Fröhlich F, McCormick DA. Endogenous electric fields may guide neocortical network activity. Neuron. 2010; 67: 129–143.
[88] Anastassiou CA, Perin R, Markram H, Koch C. Ephaptic coupling of cortical neurons. Nature Neuroscience. 2011; 14: 217–223.
[89] Coste B, Xiao B, Santos JS, Syeda R, Grandl J, Spencer KS, *et al*. Piezo proteins are pore-forming subunits of mechanically activated channels. Nature. 2012; 483: 176–181.
[90] Shin KC, Park HJ, Kim JG, Lee IH, Cho H, Park C, *et al*. The Piezo2 ion channel is mechanically activated by low-threshold positive pressure. Scientific Reports. 2019; 9: 6446.
[91] McCarter GC, Reichling DB, Levine JD. Mechanical transduction by rat dorsal root ganglion neurons in vitro. Neuroscience Letters. 1999; 273: 179–182.
[92] de Oliveira RB, Howlett MCH, Gravina FS, Imtiaz MS, Callister RJ, Brichta AM, *et al*. Pacemaker currents in mouse locus coeruleus neurons. Neuroscience. 2010; 170: 166–177.
[93] Zeppilli S, Ackels T, Attey R, Klimpert N, Ritola KD, Boeing S, *et al*. Molecular characterization of projection neuron subtypes in the mouse olfactory bulb. eLife. 2021; 10: e65445.
[94] Grosmaitre X, Santarelli LC, Tan J, Luo M, Ma M. Dual functions of mammalian olfactory sensory neurons as odor detectors and mechanical sensors. Nature Neuroscience. 2007; 10: 348–354.
[95] Connelly T, Yu Y, Grosmaitre X, Wang J, Santarelli LC, Savigner A, *et al*. G protein-coupled odorant receptors underlie mechanosensitivity in mammalian olfactory sensory neurons. Proceedings of the National Academy of Sciences of the United States of America. 2015; 112: 590–595.
[96] Moberly AH, Schreck M, Bhattarai JP, Zweifel LS, Luo W, Ma M. Olfactory inputs modulate respiration-related rhythmic activity in the prefrontal cortex and freezing behavior. Nature Communications. 2018; 9: 1528.
[97] Chesler AT, Szczot M, Bharucha-Goebel D, Čeko M, Donkervoort S, Laubacher C, *et al*. The Role of PIEZO2 in Human Mechanosensation. The New England Journal of Medicine. 2016; 375: 1355–1364.
[98] Florez-Paz D, Bali KK, Kuner R, Gomis A. A critical role for Piezo2 channels in the mechanotransduction of mouse proprioceptive neurons. Scientific Reports. 2016; 6: 25923.
[99] Nonomura K, Woo SH, Chang RB, Gillich A, Qiu Z, Francisco AG, *et al*. Piezo2 senses airway stretch and mediates lung inflation-induced apnoea. Nature. 2017; 541: 176–181.
[100] Chapleau MW, Hajduczok G, Abboud FM. Pulsatile activation of baroreceptors causes central facilitation of baroreflex. The American Journal of Physiology. 1989; 256: H1735–41.
[101] Chapleau MW, Hajduczok G, Abboud FM. New insights into the influence of pulsatile pressure on the arterial baroreceptor reflex. Clinical and Experimental Hypertension. Part A, Theory and Practice. 1988; 10: 179–191.
[102] Czosnyka M, Pickard JD, Steiner LA. Principles of intracranial pressure monitoring and treatment. Handbook of Clinical Neurology. 2017; 140: 67–89.
[103] Nag DS, Sahu S, Swain A, Kant S. Intracranial pressure monitoring: Gold standard and recent innovations. World Journal of Clinical Cases. 2019; 7: 1535–1553.
[104] Wagshul ME, Eide PK, Madsen JR. The pulsating brain: A review of experimental and clinical studies of intracranial pulsatility. Fluids and Barriers of the CNS. 2011; 8: 5.
[105] Cushing, H. Concerning a definitive regulatory mechanism of the vaso-motor centre which controls blood pressure during cerebral compression. Bulletin of Johns Hopkins Hospital. 1901; 12: 290–292.
[106] Doba N, Reis DJ. Localization within the lower brainstem of a receptive area mediating the pressor response to increased intracranial pressure (the Cushing response). Brain Research. 1972; 47: 487–491.
[107] Schmidt EA, Czosnyka Z, Momjian S, Czosnyka M, Bech RA, Pickard JD. Intracranial baroreflex yielding an early cushing response in human. Acta Neurochirurgica. Supplement. 2005; 95: 253–256.
[108] Paton JFR, Dickinson CJ, Mitchell G. Harvey Cushing and the regulation of blood pressure in giraffe, rat and man: introducing 'Cushing's mechanism'. Experimental Physiology. 2009; 94: 11–17.
[109] Guild SJ, Saxena UA, McBryde FD, Malpas SC, Ramchandra R. Intracranial pressure influences the level of sympathetic tone. American Journal of Physiology. Regulatory, Integrative and Comparative Physiology. 2018; 315: R1049–R1053.

[110] Schmidt EA, Despas F, Pavy-Le Traon A, Czosnyka Z, Pickard JD, Rahmouni K, *et al*. Intracranial Pressure Is a Determinant of Sympathetic Activity. Frontiers in Physiology. 2018; 9: 11.
[111] Angelova PR, Kasymov V, Christie I, Sheikhbahaei S, Turovsky E, Marina N, *et al*. Functional Oxygen Sensitivity of Astrocytes. The Journal of Neuroscience. 2015; 35: 10460–10473.
[112] Mastitskaya S, Turovsky E, Marina N, Theparambil SM, Hadjihambi A, Kasparov S, *et al*. Astrocytes Modulate Baroreflex Sensitivity at the Level of the Nucleus of the Solitary Tract. The Journal of Neuroscience. 2020; 40: 3052–3062.
[113] Marina N, Christie IN, Korsak A, Doronin M, Brazhe A, Hosford PS, *et al*. Astrocytes monitor cerebral perfusion and control systemic circulation to maintain brain blood flow. Nature Communications. 2020; 11: 131.
[114] Takizawa K, Matsumae M, Sunohara S, Yatsushiro S, Kuroda K. Characterization of cardiac- and respiratory-driven cerebrospinal fluid motion based on asynchronous phase-contrast magnetic resonance imaging in volunteers. Fluids and Barriers of the CNS. 2017; 14: 25.
[115] Vinje V, Ringstad G, Lindstrøm EK, Valnes LM, Rognes ME, Eide PK, *et al*. Respiratory influence on cerebrospinal fluid flow - a computational study based on long-term intracranial pressure measurements. Scientific Reports. 2019; 9: 9732.
[116] Yamada S, Miyazaki M, Yamashita Y, Ouyang C, Yui M, Nakahashi M, *et al*. Influence of respiration on cerebrospinal fluid movement using magnetic resonance spin labeling. Fluids and Barriers of the CNS. 2013; 10: 36.
[117] Aktas G, Kollmeier JM, Joseph AA, Merboldt KD, Ludwig HC, Gärtner J, *et al*. Spinal CSF flow in response to forced thoracic and abdominal respiration. Fluids and Barriers of the CNS. 2019; 16: 10.
[118] Kollmeier JM, Gürbüz-Reiss L, Sahoo P, Badura S, Ellebracht B, Keck M, *et al*. Deep breathing couples CSF and venous flow dynamics. Scientific Reports. 2022; 12: 2568.
[119] Soellinger M, Rutz AK, Kozerke S, Boesiger P. 3D cine displacement-encoded MRI of pulsatile brain motion. Magnetic Resonance in Medicine. 2009; 61: 153–162.
[120] Feinberg DA, Mark AS. Human brain motion and cerebrospinal fluid circulation demonstrated with MR velocity imaging. Radiology. 1987; 163: 793–799.
[121] Lunkenheimer PP, Redmann K, Florek J, Fassnacht U, Cryer CW, Wübbeling F, *et al*. The forces generated within the musculature of the left ventricular wall. Heart. 2004; 90: 200–207.
[122] Alperin N. Does the brain have mechanical compliance? Magma. 2020; 33: 753–756.
[123] Tenti G, Sivaloganathan S, Drake JM. The synchrony of arterial and CSF pulsations is not due to resonance. Pediatric Neurosurgery. 2002; 37: 221–222.
[124] Tenti G, Sivaloganathan S, Drake JM. Mathematical modeling of the brain: principles and challenges. Neurosurgery. 2008; 62: 1146–1162.
[125] Egnor M, Rosiello A, Zheng L. A model of intracranial pulsations. Pediatric Neurosurgery. 2001; 35: 284–298.
[126] Egnor M, Wagshul M, Zheng L, Rosiello A. Resonance and the synchrony of arterial and CSF pulsations. Pediatric Neurosurgery. 2003; 38: 273–276.
[127] Egnor M. The cerebral windkessel as a dynamic pulsation absorber. BIO-Complexity. 2019; 3: 1–35.
[128] Belz GG. Elastic properties and Windkessel function of the human aorta. Cardiovascular Drugs and Therapy. 1995; 9: 73–83.
[129] Wagshul ME, Kelly EJ, Yu HJ, Garlick B, Zimmerman T, Egnor MR. Resonant and notch behavior in intracranial pressure dynamics. Journal of Neurosurgery. Pediatrics. 2009; 3: 354–364.
[130] Luecke S. Freediving neurophenomenology and skilled action: an investigation of brain, body, and behavior through breath. Phenomenology and the Cognitive Sciences. 2022; 1–37.
[131] McKnight JC, Mulder E, Ruesch A, Kainerstorfer JM, Wu J, Hakimi N, *et al*. When the human brain goes diving: using near-infrared spectroscopy to measure cerebral and systemic cardiovascular responses to deep, breath-hold diving in elite freedivers. Philosophical Transactions of the Royal Society of London. Series B, Biological Sciences. 2021; 376: 20200349.
[132] McBride DW, Jr, Hamill OP. Pressure-clamp: a method for rapid step perturbation of mechanosensitive channels. Pflugers Archiv: European Journal of Physiology. 1992; 421: 606–612.
[133] McBride DW, Jr, Hamill OP. Pressure-clamp technique for measurement of the relaxation kinetics of mechanosensitive channels. Trends in Neurosciences. 1993; 16: 341–345.
[134] McBride DW Jr, Hamill OP. A fast pressure clamp technique for studying mechano-gated channels. In Sakmann B, Neher E (eds.) Single channel recording (pp. 329–340). 2nd edn. Plenum: New York. 1995.
[135] Hamill OP, McBride DW, Jr. Rapid adaptation of single mechanosensitive channels in Xenopus oocytes. Proceedings of the National Academy of Sciences of the United States of America. 1992; 89: 7462–7466.
[136] Hamill OP, McBride DW, Jr. Induced membrane hypo/hypermechanosensitivity: a limitation of patch-clamp recording. Annual Review of Physiology. 1997; 59: 621–631.
[137] Besch SR, Suchyna T, Sachs F. High-speed pressure clamp. Pflugers Archiv: European Journal of Physiology. 2002; 445: 161–166.
[138] Hao J, Ruel J, Coste B, Roudaut Y, Crest M, Delmas P. Piezoelectrically driven mechanical stimulation of sensory neurons. Methods in Molecular Biology. 2013; 998: 159–170.
[139] Lewis AH, Cui AF, McDonald MF, Grandl J. Transduction of Repetitive Mechanical Stimuli by Piezo1 and Piezo2 Ion Channels. Cell Reports. 2017; 19: 2572–2585.
[140] Zhang Y, Gao F, Popov VL, Wen JW, Hamill OP. Mechanically gated channel activity in cytoskeleton-deficient plasma membrane blebs and vesicles from Xenopus oocytes. The Journal of Physiology. 2000; 523: 117–130.
[141] Lewis AH, Grandl J. Mechanical sensitivity of Piezo1 ion channels can be tuned by cellular membrane tension. eLife. 2015; 4: e12088.
[142] Syeda R, Florendo MN, Cox CD, Kefauver JM, Santos JS, Martinac B, *et al*. Piezo1 Channels Are Inherently Mechanosensitive. Cell Reports. 2016; 17: 1739–1746.
[143] Cox CD, Bae C, Ziegler L, Hartley S, Nikolova-Krstevski V, Rohde PR, *et al*. Removal of the mechanoprotective influence of the cytoskeleton reveals PIEZO1 is gated by bilayer tension. Nature Communications. 2016; 7: 10366.
[144] Wang J, Jiang J, Yang X, Zhou G, Wang L, Xiao B. Tethering Piezo channels to the actin cytoskeleton for mechanogating via the cadherin-β-catenin mechanotransduction complex. Cell Reports. 2022; 38: 110342.
[145] Loukin S, Zhou X, Su Z, Saimi Y, Kung C. Wild-type and brachyolmia-causing mutant TRPV4 channels respond directly to stretch force. The Journal of Biological Chemistry. 2010; 285: 27176–27181.
[146] Raisinghani M, Premkumar LS. Block of native and cloned vanilloid receptor 1 (TRPV1) by aminoglycoside antibiotics. Pain. 2005; 113: 123–133.
[147] Delmas P, Hao J, Rodat-Despoix L. Molecular mechanisms of mechanotransduction in mammalian sensory neurons. Nature Reviews. Neuroscience. 2011; 12: 139–153.
[148] Johansson RS, Vallbo AB. Tactile sensibility in the human hand: relative and absolute densities of four types of mechanoreceptive units in glabrous skin. The Journal of Physiology. 1979; 286: 283–300.
[149] McKeon B, Burke D. Component of muscle spindle discharge

related to arterial pulse. Journal of Neurophysiology. 1981; 46: 788–796.
[150] Gandevia SC, Burke D. Effect of training on voluntary activation of human fusimotor neurons. Journal of Neurophysiology. 1985; 54: 1422–1429.
[151] Douglass JK, Wilkens L, Pantazelou E, Moss F. Noise enhancement of information transfer in crayfish mechanoreceptors by stochastic resonance. Nature. 1993; 365: 337–340.
[152] Cordo P, Inglis JT, Verschueren S, Collins JJ, Merfeld DM, Rosenblum S, *et al*. Noise in human muscle spindles. Nature. 1996; 383: 769–770.
[153] Collins JJ, Imhoff TT, Grigg P. Noise-enhanced tactile sensation. Nature. 1996; 383: 770.
[154] Hô N, Destexhe A. Synaptic background activity enhances the responsiveness of neocortical pyramidal neurons. Journal of Neurophysiology. 2000; 84: 1488–1496.
[155] Linkenkaer-Hansen K, Nikulin VV, Palva S, Ilmoniemi RJ, Palva JM. Prestimulus oscillations enhance psychophysical performance in humans. The Journal of Neuroscience. 2004; 24: 10186–10190.
[156] Grund M, Al E, Pabst M, Dabbagh A, Stephani T, Nierhaus T, *et al*. Respiration, Heartbeat, and Conscious Tactile Perception. The Journal of Neuroscience. 2022; 42: 643–656.
[157] Chaudakshetrin P, Kumar VP, Satku K, Pho RW. The arteriovenous pattern of the distal digital segment. Journal of Hand Surgery. 1988; 13: 164–166.
[158] Duvernoy HM, Delon S, Vannson JL. Cortical blood vessels of the human brain. Brain Research Bulletin. 1981; 7: 519–579.
[159] Wang J, La JH, Hamill OP. *PIEZO1* Is Selectively Expressed in Small Diameter Mouse DRG Neurons Distinct From Neurons Strongly Expressing *TRPV1*. Frontiers in Molecular Neuroscience. 2019; 12: 178.
[160] Shin SM, Moehring F, Itson-Zoske B, Fan F, Stucky CL, Hogan QH, *et al*. Piezo2 mechanosensitive ion channel is located to sensory neurons and nonneuronal cells in rat peripheral sensory pathway: implications in pain. Pain. 2021; 162: 2750–2768.
[161] Delmas P, Parpaite T, Coste B. PIEZO channels and newcomers in the mammalian mechanosensitive ion channel family. Neuron. 2022; 110: 2713–2727.
[162] Berthoud HR, Neuhuber WL. Functional and chemical anatomy of the afferent vagal system. Autonomic Neuroscience: Basic & Clinical. 2000; 85: 1–17.
[163] Benarroch EE. The central autonomic network: functional organization, dysfunction, and perspective. Mayo Clinic Proceedings. 1993; 68: 988–1001.
[164] Craig AD. How do you feel? Interoception: the sense of the physiological condition of the body. Nature Reviews. Neuroscience. 2002; 3: 655–666.
[165] Pollatos O, Kirsch W, Schandry R. Brain structures involved in interoceptive awareness and cardioafferent signal processing: a dipole source localization study. Human Brain Mapping. 2005; 26: 54–64.
[166] Gray MA, Taggart P, Sutton PM, Groves D, Holdright DR, Bradbury D, *et al*. A cortical potential reflecting cardiac function. Proceedings of the National Academy of Sciences of the United States of America. 2007; 104: 6818–6823.
[167] Dampney RAL. Central neural control of the cardiovascular system: current perspectives. Advances in Physiology Education. 2016; 40: 283–296.
[168] MacKinnon S, Gevirtz R, McCraty R, Brown M. Utilizing heartbeat evoked potentials to identify cardiac regulation of vagal afferents during emotion and resonant breathing. Applied Psychophysiology and Biofeedback. 2013; 38: 241–255.
[169] Moore CI, Cao R. The hemo-neural hypothesis: on the role of blood flow in information processing. Journal of Neurophysiology. 2008; 99: 2035–2047.
[170] Kim KJ, Ramiro Diaz J, Iddings JA, Filosa JA. Vasculo-Neuronal Coupling: Retrograde Vascular Communication to Brain Neurons. The Journal of Neuroscience. 2016; 36: 12624–12639.
[171] Thayer JF, Hansen AL, Saus-Rose E, Johnsen BH. Heart rate variability, prefrontal neural function, and cognitive performance: the neurovisceral integration perspective on self-regulation, adaptation, and health. Annals of Behavioral Medicine. 2009; 37: 141–153.
[172] Zaccaro A, Perrucci MG, Parrotta E, Costantini M, Ferri F. Brain-heart interactions are modulated across the respiratory cycle via interoceptive attention. NeuroImage. 2022; 262: 119548.
[173] Shaffer F, McCraty R, Zerr CL. A healthy heart is not a metronome: an integrative review of the heart's anatomy and heart rate variability. Frontiers in Psychology. 2014; 5: 1040.
[174] Elstad M, Toska K, Chon KH, Raeder EA, Cohen RJ. Respiratory sinus arrhythmia: opposite effects on systolic and mean arterial pressure in supine humans. The Journal of Physiology. 2001; 536: 251–259.
[175] Yasuma F, Hayano JI. Respiratory sinus arrhythmia: why does the heartbeat synchronize with respiratory rhythm? Chest. 2004; 125: 683–690.
[176] Skytioti M, Elstad M. Respiratory Sinus Arrhythmia is Mainly Driven by Central Feedforward Mechanisms in Healthy Humans. Frontiers in Physiology. 2022; 13: 768465.
[177] Pfurtscheller G, Rassler B, Schwerdtfeger AR, Klimesch W, Andrade A, Schwarz G, *et al*. "Switch-Off" of Respiratory Sinus Arrhythmia May Be Associated With the Activation of an Oscillatory Source (Pacemaker) in the Brain Stem. Frontiers in Physiology. 2019; 10: 939.
[178] Young HA, Benton D. Heart-rate variability: a biomarker to study the influence of nutrition on physiological and psychological health? Behavioural Pharmacology. 2018; 29: 140–151.
[179] Lehrer PM, Vaschillo E, Vaschillo B, Lu SE, Eckberg DL, Edelberg R, *et al*. Heart rate variability biofeedback increases baroreflex gain and peak expiratory flow. Psychosomatic Medicine. 2003; 65: 796–805.
[180] McCraty R. Following the Rhythm of the Heart: HeartMath Institute's Path to HRV Biofeedback. Applied Psychophysiology and Biofeedback. 2022; 47: 305–316.
[181] Chang C, Cunningham JP, Glover GH. Influence of heart rate on the BOLD signal: the cardiac response function. NeuroImage. 2009; 44: 857–869.
[182] Hu X, Nenov V, Vespa P, Bergsneider M. Characterization of interdependency between intracranial pressure and heart variability signals: a causal spectral measure and a generalized synchronization measure. IEEE Transactions on Bio-medical Engineering. 2007; 54: 1407–1417.
[183] Fedriga M, Czigler A, Nasr N, Zeiler FA, Park S, Donnelly J, *et al*. Autonomic Nervous System Activity during Refractory Rise in Intracranial Pressure. Journal of Neurotrauma. 2021; 38: 1662–1669.
[184] Draguhn A, Sauer JF. Body and mind: how somatic feedback signals shape brain activity and cognition. Pflugers Archiv: European Journal of Physiology. 2023; 475: 1–4.
[185] Folschweiller S, Sauer JF. Controlling neuronal assemblies: a fundamental function of respiration-related brain oscillations in neuronal networks. Pflugers Archiv: European Journal of Physiology. 2023; 475: 13–21.
[186] Lakatos P, Shah AS, Knuth KH, Ulbert I, Karmos G, Schroeder CE. An oscillatory hierarchy controlling neuronal excitability and stimulus processing in the auditory cortex. Journal of Neurophysiology. 2005; 94: 1904–1911.
[187] Klimesch W. The frequency architecture of brain and brain body oscillations: an analysis. European Journal of Neuro-

science. 2018; 48: 2431–2453.
[188] Pletzer B, Kerschbaum H, Klimesch W. When frequencies never synchronize: the golden mean and the resting EEG. Brain Research. 2010; 1335: 91–102.
[189] Rassi E, Dorffner G, Gruber W, Schabus M, Klimesch W. Coupling and Decoupling between Brain and Body Oscillations. Neuroscience Letters. 2019; 711: 134401.
[190] Buzsáki G, Logothetis N, Singer W. Scaling brain size, keeping timing: evolutionary preservation of brain rhythms. Neuron. 2013; 80: 751–764.
[191] Claude B. Lecture on the physiology of the heart and its connections with the brain, delivered at the Sorbonne, the 27th March, 1865. Savannah: Purse. 1867.
[192] Critchley HD, Harrison NA. Visceral influences on brain and behavior. Neuron. 2013; 77: 624–638.
[193] Elmegaard SL, Johnson M, Madsen PT, McDonald BI. Cognitive control of heart rate in diving harbor porpoises. Current Biology. 2016; 26: R1175–R1176.
[194] Hsueh B, Chen R, Jo Y, Tang D, Raffiee M, Kim YS, *et al*. Cardiogenic control of affective behavioural state. Nature. 2023; 615: 292–299.
[195] Lee AK, Manns ID, Sakmann B, Brecht M. Whole-cell recordings in freely moving rats. Neuron. 2006; 51: 399–407.
[196] Frysinger RC, Harper RM. Cardiac and respiratory correlations with unit discharge in human amygdala and hippocampus. Electroencephalography and Clinical Neurophysiology. 1989; 72: 463–470.
[197] Frysinger RC, Harper RM. Cardiac and respiratory relationships with neural discharge in the anterior cingulate cortex during sleep-walking states. Experimental Neurology. 1986; 94: 247–263.
[198] Massimini M, Porta A, Mariotti M, Malliani A, Montano N. Heart rate variability is encoded in the spontaneous discharge of thalamic somatosensory neurones in cat. The Journal of Physiology. 2000; 526: 387–396.
[199] Hamill OP, Huguenard JR, Prince DA. Patch-clamp studies of voltage-gated currents in identified neurons of the rat cerebral cortex. Cerebral Cortex. 1991; 1: 48–61.
[200] Young BA, Cramberg MJ. Treadmill locomotion in the American alligator (Alligator mississippiensis) produces dynamic changes in intracranial cerebrospinal fluid pressure. Scientific Reports. 2022; 12: 11826.
[201] Gaskell WH. On a segmental group of ganglion cells in the spinal cord of the alligator. The Journal of Physiology. 1885; 7: 19–30.
[202] Grillner S, Williams T, Lagerbäck PA. The edge cell, a possible intraspinal mechanoreceptor. Science. 1984; 223: 500–503.
[203] Donald D. On the incidence and locations of nerve cells in the spinal white matter of two species of primates, man and the cynomolgus monkey. The Journal of Comparative Neurology. 1953; 99: 103–115.
[204] Picton LD, Bertuzzi M, Pallucchi I, Fontanel P, Dahlberg E, Björnfors ER, *et al*. A spinal organ of proprioception for integrated motor action feedback. Neuron. 2021; 109: 1188–1201.e7.
[205] Salameh LJ, Bitzenhofer SH, Hanganu-Opatz IL, Dutschmann M, Egger V. Blood pressure pulsations modulate olfactory bulb neuronal activity via mechanosensitive ion channels. bioRxiv. 2023; 7: 550787.